MIT Open Access Articles

MIGHT BE A DUPLICATE: 30 years of advances in functionalization of carbon nanomaterials for biomedical applications: a practical review

Massachusetts Institute of Technology

JMR EARLY CAREER SCHOLARS IN MATERIALS SCIENCE ANNUAL ISSUE: REVIEW

30 years of advances in functionalization of carbon nanomaterials for biomedical applications: a practical review

Neelkanth M. Bardhan[a)]
Department of Materials Science and Engineering, Department of Biological Engineering, Koch Institute for Integrative Cancer Research, Massachusetts Institute of Technology, Cambridge, MA 02139, USA

Carbon-based nanomaterials (CANOMATs), including fullerenes, carbon nanotubes, graphene, and their derivatives, are widely considered to be the next-generation materials for a broad range of biomedical applications, owing to their unique opto-electronic, chemical, and mechanical properties. However, for bio-applications, CANOMATs need to be surface-functionalized, to render them passive, non-toxic, and water-soluble. Here, we review the current state-of-the-art in the methods of functionalization of CANOMATs. In contrast to other Reviews, we present an objective analysis of the various approaches reported in the literature, using metrics such as the agent of functionalization, number of steps, and time required, the need for special instruments, effect on properties, scalability, reproducibility, and applications. Our Review offers a way for researchers to make a rational selection of the process of functionalization to best suit their desired application. This opens up new opportunities for developing targeted functionalization strategies, based on the need to excel at the above metrics.

Dr. Neelkanth M. Bardhan (Neel) did his undergraduate in materials science, with a Bachelor of Technology from the Indian Institute of Technology (IIT) Bombay in Mumbai, India. He then did his Ph.D. in Materials Science and Engineering from the Massachusetts Institute of Technology in Cambridge, MA, USA. For his Ph.D. research on the use of biologically templated, carbon-based nanomaterials for biosensing and diagnostic applications, Neel was a recipient of the 2015 MRS Graduate Student Gold Award, awarded by the Materials Research Society in April 2015. Neel is currently a dual fellow, funded by the 2016 Misrock Postdoctoral Fellowship, and the RLE Translational Fellows Program, working toward clinical translation of his nanotechnology-based approach to cancer imaging. Besides research, Neel is actively involved in leadership; influencing issues pertaining to science funding, climate change, and sustainability, and outreach. He is a big admirer of cats, and looks to them for his engineering inspiration.

Neelkanth M. Bardhan

I. INTRODUCTION

In the past 30 years, there has been explosive growth in interest in the use of carbon-based nanomaterials, ever since the introduction of 0D (C_{60} buckminsterfullerene),[1] 1D (carbon nanotubes),[2] and 2D (graphene)[3] forms (Fig. 1) of CArbon-based NanO MATerials (CANOMATs), in that chronological order, where D refers to the dimensionality. These low-D CANOMATs are exceptionally advantageous for biomedical applications, because of their unique opto-electronic, chemical, mechanical, and physical properties and their large surface area,[4–7] coupled with dimensions

that are comparable to those of biomolecules such as DNA or proteins.[8] For a brief overview of the properties of pristine CANOMATs, the reader is referred to the Supplementary Material. What makes these materials challenging to use is that the protocols for synthesis of carbon nanomaterials result in large dispersion in the purity, yield, and consequently the physico-chemical properties of these materials. Since physiological responses in biological conditions are highly sensitive to uniformity and reproducibility of the material properties, some purification and surface functionalization steps are necessary. Further, to achieve biocompatibility and water solubility, CANOMATs need to be surface-functionalized.

While there have been many reviews[9–23] over the years on the use of CANOMATs for biological applications (focusing on aspects such as biological sensing, imaging,
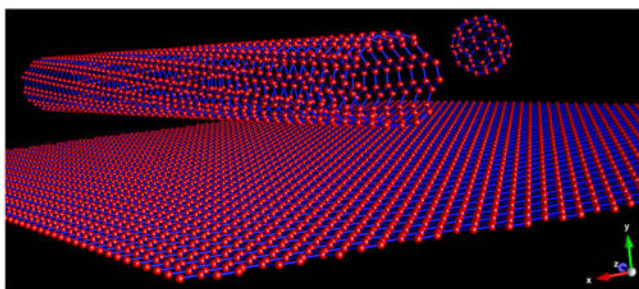
FIG. 1. The beauty of carbon. Schematic showing the hexagonal lattice structure of the most common forms of CANOMATs: a semi-infinite sheet of graphene (2D), a single-walled carbon nanotube of (6, 5) chirality (1D), and a C_{60} bucky ball (0D). The red spheres represent C atoms. Rendered using VESTA.[155]

drug delivery, and therapy), to the best of our knowledge, there have been no comprehensive reviews comparing the various strategies for the functionalization of these materials. This is an especially important consideration for early-career scholars and researchers in the materials science community. Although there is great variety[24–31] in the availability of functionalization schemes for CANOMATs, young investigators are often faced with the challenging optimization problem of deciding on a technique which is suitable for their particular application, while satisfying the following constraints: (i) agent of functionalization; (ii) number of steps and time required to develop; (iii) the availability of necessary instruments; (iv) the desirability of material properties affected by the functionalization; (v) the scalability of the approach; (vi) reproducibility (both by the originators of the technique, and by subsequent researchers); and (vii) the application space which has already been explored. The details about the parameters used for this Review are listed in the Supplementary Material.

This Review aims to aggregate the various approaches used for functionalization of carbon-based nanomaterials, including chemical and biological functionalization approaches. The parameters used in this Review are discussed in the Supplementary Material. We discuss examples of the Belcher group's work [Figs. 4(a)–4(c), 7(a), 7(b) and 8(g)] on the use of a biological template (M13 bacteriophage), as a scaffold for noncovalent functionalization of carbon nanotubes for detection of cancers[32,33] and infectious diseases,[34] and also the use of physical or chemical modification to functionalize graphene oxide (GO) for biosensing applications[35] involving cell capture from whole blood; using the same metrics described above. The goal of this Review is to provide an objective, quantitative (wherever possible) comparison of these parameters, to help researchers make an informed decision while choosing a functionalization technique for their desired application.

II. FUNCTIONALIZATION OF FULLERENES

A summary of the various techniques of functionalization used for fullerenes is presented in Table 1 in the Supplementary Material.

A. Non-covalent functionalization of fullerenes

Fullerenes are notoriously hard to solubilize in most solvents[36] (let alone aqueous dispersion). Variations in temperature and pressure are required to solubilize fullerenes. The solubility of C_{60} shows a maximum in solvents such as CS_2, toluene, and hexane at ∼280 K. Given these challenges, it would appear reasonable that most approaches to functionalizing fullerenes have relied on chemical modification through covalent bonding. Nevertheless, there are a few reports of non-covalent functionalization on fullerene molecules.

Manna, A.K. et al.[37] have performed first-principle density functional theory (DFT) calculations on the effect of non-covalent interactions of fullerenes (C_{60}, C_{70}, C_{80} and B_{80}) with single-layer graphene. Their calculations suggest that larger fullerenes result in greater binding strength, facilitated by van der Waals interactions between the adsorbed fullerene and graphene [Fig. 2(a)]. All graphene–fullerene composites displayed perfectly metallic behavior. Besides graphene, several groups of researchers have attempted to form stable polymer composites with fullerenes through non-covalent interactions. For example, Jung, S. et al.[38] studied the interaction between protonated porphyrin and fullerenes (C_{60} and C_{70}) in the gas phase, synthesized by electrospray ionization of the porphyrin–fullerene mixture. C_{70} was shown to bind more strongly than C_{60}, in agreement with the DFT results discussed above. It was rationalized that the protonated porphyrin–fullerene complex is stabilized by π–π interactions. In another manifestation of electron donor–acceptor interactions, Teh, S-L. et al.[39] have demonstrated the dispersion of C_{60} in a polymer matrix, Fig. 2(c). Subsequently, Li, F. et al.[40] developed polymer/fullerene nanofibers through cooperative non-covalent interaction, by reacting a diblock copolymer derivative of poly(3-hexylthiophene) (P3HT) and phenyl-C_{61}-butyric acid methyl ester (PCBM), with improved performance in organic photovoltaic (OPV) devices. Recently, Reddy, B.K. et al.[41] studied the crystal structure of fullerenes complexed with antiaromatic isophlorin molecules (a tetra-pyrrolic macrocyclic compound, with a structure similar to porphyrin). They concluded that the complex is stabilized owing to the favored van der Waals interaction of the curved π-surface of the C_{60} molecule with the nearly planar surface of the anti-aromatic π-surface of the isophlorin molecules [Fig. 2(b)]. Basiuk, V.A. et al.[42] reported that upon calculating the binding energies of 20 L-amino acids with C_{60}, they found poor correlation between the binding energies and the scale of
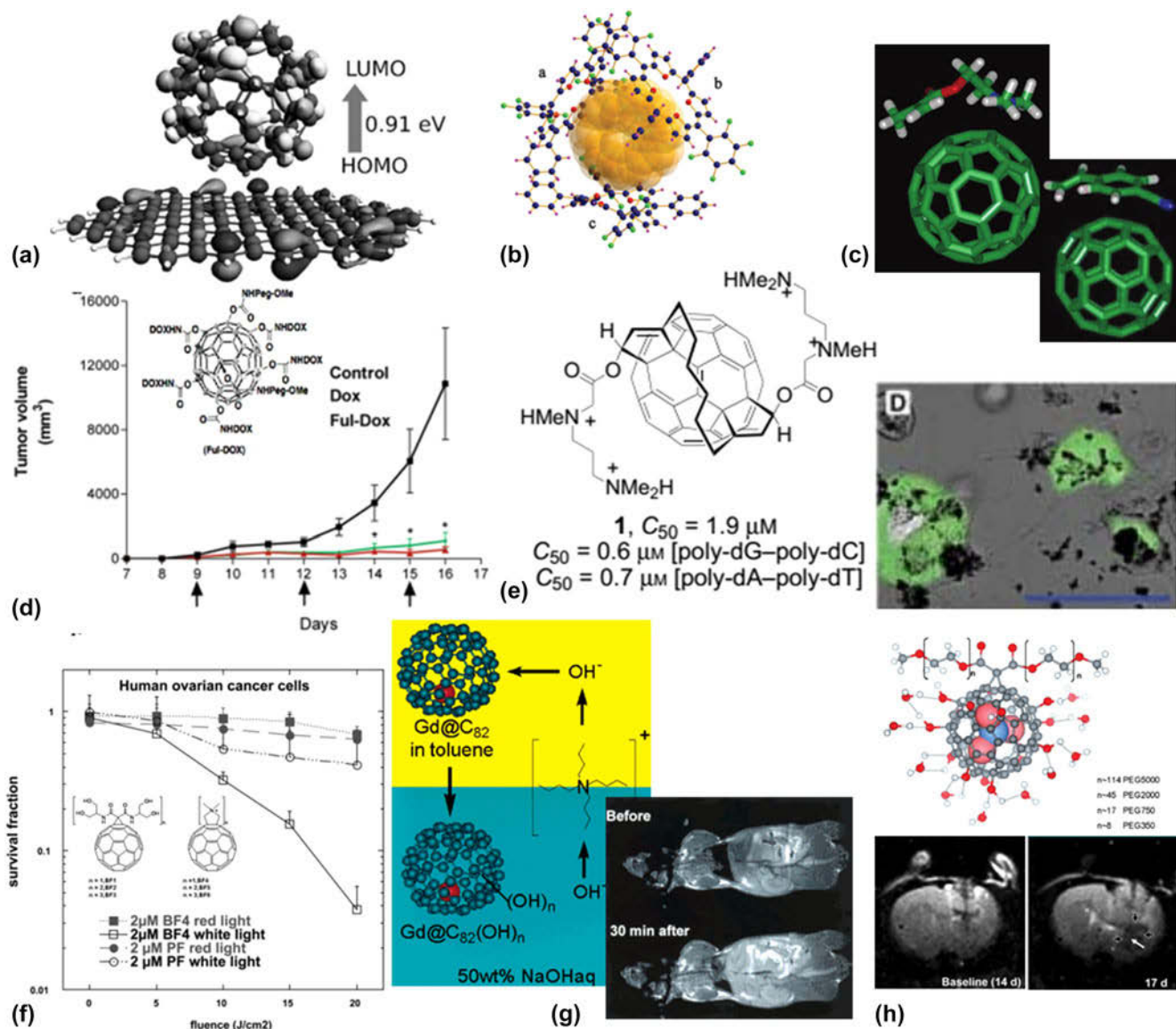
FIG. 2. Covalent and non-covalent functionalization of fullerenes. (a) DFT calculation of the molecular orbital separation between C_{60} adsorbed on the graphene sheet, indicating stability by van der Waals interactions. (b) Triplet molecular complex of anti-aromatic tetraoxaisophlorin complexed with C_{60} in a prismatic arrangement. (c) Optimized geometries of C_{60}-polymer composites of DMAEMA or CNSt, resulting from non-covalent electron donor–acceptor interactions. (d) *In vivo* efficacy of tumor treatment, using fullerene–doxorubicin conjugates, in a melanoma mouse model. Inset shows the structure of the molecule used. (e) 2-handed amphiphilic fullerene, used for the delivery of DNA. Inset shows transfected cells expressing GFP. (f) PDT-mediated killing of ovarian cancer cells, with superior performance of the BF4 fullerene derivative compared to photofrin (PF), a commercial sensitizer. (g) Synthesis procedure for the water-soluble gadofullerenes. Inset shows T_1-weighted MRI, showing strong accumulation in the RES system, at $\sim 1/20$ of the dose of commercial MR contrast agents. (h) Water-soluble, endohedral trimetallic nitride gadofullerenes, functionalized with PEG (top). T_2-weighted MR imaging of brain tumor (bottom panel, white arrow) in rat. See text for definitions of molecules. Reprinted with permissions from: (a and e) Manna and Pati,[37] Nakamura et al.[49] © 2013, 2000 John Wiley and Sons, respectively. (b) Reddy et al.[41] (c, d, g, and h top) Teh et al.,[39] Chaudhuri et al.,[46] Mikawa et al.,[56] Zhang et al.,[61] © 2011, 2009, 2001, 2010 American Chemical Society, respectively. (f) Mroz et al.[53] © 2007 Royal Society of Chemistry. (h, bottom panel) Fatouros et al.[60] © 2006 Radiological Society of North America.

hydrophobicity proposed by other research groups. More work needs to be done to understand the mechanism (or possibly a combination of mechanisms) of interaction of the bucky ball with adsorbed molecules.

B. Covalent functionalization of fullerenes

Among the first of the CANOMATs to be discovered, fullerene chemistry has been thoroughly investigated and studied.[43] A large number of the functionalization

schemes subsequently applied to carbon nanotubes and graphene trace their roots back to the methods used for functionalization of fullerenes.

1. Oxidation and hydroxylation

Fullerenes can also be oxidized with reagents such as OsO_4, ozone, oxone monopersulfate, and 3-chloroperoxy benzoic acid, to name a few. In fact, the reaction of OsO_4 causes an adduct, $C_{60}(OsO_4)$ (4-*tert*-butylpyridine)$_2$, which breaks the cage structure, and can be detected in x-ray crystallography, which was one of the original confirmations[44] used in the determination of the buckyball framework. Similarly, poly-hydroxylated derivatives, called "fullerenols" or "fullerols", $C_{60}(OH)_{8-40}$ have been synthesized using fullerene reactions with dilute H_2SO_4 and KNO_3, or with dilute NaOH in the presence of H_2O_2 or other peroxides.

In terms of applications, functionalized fullerenes have been studied extensively for their potential use in drug delivery, photodynamic therapy (reactive oxygen species generation), and in targeted imaging. For example, fullerenol, $C_{60}(OH)_{24}$ has been shown to protect liver and heart tissue, from the chronic toxicity effects of administering doxorubicin, a chemotherapy agent, in male Wistar rats being treated for colorectal cancer, by Injac, R. et al.[45] Chaudhuri, P. et al.[46] have shown that fullerenol complexed with doxorubicin can suppress the proliferation of cancer [Fig. 2(d)] by a G2-M cell cycle block, resulting in apoptosis, with *in vivo* efficacy comparable to that of the free drug, without the systemic toxicity side effects. Partha, R. et al.[47] have formulated "buckysomes", analogous to liposomes used for the delivery of hydrophobic drugs and other molecules. Amphiphilic fullerene structures embedded with the hydrophobic anticancer drug, paclitaxel (PTX), resulted in *in vitro* therapeutic efficacy (toward MCF-7 breast cancer cells) comparable to that of a commercial formulation of the drug. Similarly, Liu, J-H. et al.[48] have characterized a fullerene–DOX conjugate to be stoichiometrically well-defined, and studied its uptake in MCF-7 cells. They determined that the lipophilic fullerene–DOX conjugate accumulates predominantly in the cytoplasm (unlike free DOX, which proliferates into the nucleus), and may be contributing to cell toxicity through other mechanisms (structural damage to mitochondria, non protein-associated DNA strand break, or the generation of cytotoxic free radical species). Several groups of researchers have attempted to use functionalized fullerenes as gene delivery vehicles. For example, Nakamura, E. et al.[49] synthesized two-handed tetramine-conjugated fullerene, which binds to duplex DNA in a reversible manner, which is internalized into cells by phagocytosis. The efficiency of transfection of a GFP-expression vector [Fig. 2(e)] was determined to

be comparable to that of commercial reagents. Building on this approach based on tetramino fullerene, Maeda-Mamiya, R. et al.[50] developed an *in vivo* gene delivery system to deliver the insulin-2 gene, with consequent reduction in blood glucose levels in a mouse model.

Photodynamic therapy is another active area of research where fullerene derivatives play an important role. For example, Tokayuma, H. et al.[51] showed that fullerene carboxylic acid, a water-miscible derivative, is biochemically active under low-energy light. As a photosensitive molecule, it was shown to have enhanced cytotoxicity in vitro against HeLa S3 cancer cells, as well as an ability to cleave DNA selectively at the G-sites, in a 182 base-pair fragment. In another approach, Liu, J. et al.[52] have fabricated a photosensitizer with magnetic resonance activity, to enable photodynamic therapy of tumors, by chelating Gd^{3+} to PEG-functionalized C_{60}. The PDT efficacy of this construct was compared to that of Magnevist, a commercial MRI formulation of gadopentetic acid, in a murine tumor model, and was simultaneously shown to maintain an enhanced MRI signal for a longer duration in tumor tissue. A review of the work done in the area of PDT using fullerene chemistries [Fig. 2(f)] is done by Mroz, P. et al.[53] One of the main challenges that need to be overcome (in addition to obvious concerns of cytotoxicity, which are discussed in the Supplementary Material) is the absorption maxima of fullerenes being in the UV-blue part of the wavelength spectrum. This limits their use to shallow or sub-surface diseases (most commercial formulations of photosensitizers are activated in the red-IR wavelengths),[54] since tissue penetration depth is limited in these wavelength ranges due to very high attenuation[55] caused by a combination of autofluorescence, absorption, and scattering mechanisms.

Fullerenes can also be designed to act as MRI contrast agents, in the form of endohedral fullerenes encapsulating the Gd^{3+} ion inside the fullerene cage (also known as "gadofullerenes"), as pH-responsive imaging probes. The first demonstration of metallofullerenes as *in vivo* contrast agents was by Mikawa, M. et al.,[56] who synthesized water-soluble, polyhydroxyl forms, $Gd@C_{82}(OH)_{40}$ [Fig. 2(g)]. Upon i.v. administration into mice at a typical dose of ~100 μmol Gd/kg, they studied the biodistribution at 24 h, which indicated entrapment of the Gd^{3+} complex in the reticuloendothelial system (RES) organs, i.e., the lungs, liver, and spleen. This has the benefit of ~20–100% signal enhancement in these organs in the T_1-weighted mode of MRI, at 30 min post i.v. injection. In subsequent development, Bolskar, R.D. et al.[57] reported the first water-soluble contrast agent, $Gd@C_{60}[C(COOH)_2]_{10}$ with non-localizing behavior to the RES organs. The carboxylated metallofullerene showed less aggregation compared to the fullerenols, while providing relaxivity

similar to commercially available Gd^{3+}-based contrast agents. A comparative study of hydroxyl- and carboxyl-functionalized fullerenes done by Sitharaman, B. et al.[58] revealed pH-dependent agglomeration, with sizes ~30–90 nm at pH 9, to hydrodynamic diameters as large as 600–1200 nm at pH 5. In another approach, it was shown possible to encapsulate Gd^{3+} ions endohedrally by using the "trimetallic nitride template" (TNT) process proposed by Stevenson, S. et al.[59] Building on this TNT-fullerene approach, Fatouros, P.P. et al.,[60] and Zhang, J. et al.[61] have shown PEG-functionalized $Gd_3N@C_{80}[DiPEG5000(OH)_x]$ to be effective proton relaxation agents for *in vivo* tumor imaging in the rat brain [Fig. 2(h)]. As a brief footnote, fullerene derivatives have also been explored as contrast agents for X-ray imaging, such as the 2,4,6-triiodinated benzene ring substructure conjugated on to the C_{60} structure by Wharton, T. and Wilson, L.J.[62]

III. FUNCTIONALIZATION OF CARBON NANOTUBES

A summary of the various techniques of functionalization used for carbon nanotubes is presented in Table 2 in the Supplementary Material.

A. Non-covalent functionalization of carbon nanotubes

The non-covalent functionalization process has the advantage of improving the solubility of carbon nanotubes significantly, while avoiding modification of the sidewall composition. Therefore, the electronic structure of the carbon nanotubes is not perturbed to a great extent, which preserves the opto-electronic properties of the material, and makes it useful for applications such as sensing and imaging.

1. Small molecule surfactants

This is the most common class of surfactants, or stabilizing agents, used to disperse carbon nanotubes in an aqueous medium. Small-molecule surfactants, such as sodium dodecyl sulfate (SDS) or sodium cholate (SC) are amphiphilic in nature, comprising of a hydrophobic core, and a long hydrophilic tail. When the surfactant molecules are present in the dispersing medium of the CNTs at a concentration higher than the "critical micelle concentration" (CMC), they spontaneously self-assemble into micellar structures, with the hydrophobic core attached to the hydrophobic surface of the carbon nanotubes, and the hydrophilic ends sticking outward, into the aqueous medium, thereby making the wrapped CNTs form a stable suspension in water. Upon sonication, the aggregated bundles of CNTs break apart, which can then further be

wrapped with the surfactant molecules, or are eliminated from the suspension during subsequent centrifugation.

The first reported use of small molecule surfactants [Fig. 3(a)] was by O'Connell, M.J. et al.,[63] who used 1% SDS to disperse single-walled carbon nanotubes (SWNTs) in H_2O. Using this method, they were the first to report bright fluorescence from aqueous-dispersed SWNTs in the second near-infrared window (NIR-II: 900–1600 nm), which makes SWNTs ideally suited for *in vivo* biomedical imaging applications. Upon measurement of the photoluminescence spectra, they deduced the lifetime to be <2 ns, and a quantum yield ~10^{-3}, which conclusively suggested a fluorescence emission mechanism from singlet excitons. Following this exciting development, there has been a wide range of other small molecule surfactants reported to have been used for the suspension of carbon nanotubes in hydrophilic environments. Along with SDS, dodecyl-benzene sodium sulfonate (NaDDBS) is also commonly used, due to the high dispersive efficiency of the latter owing to the presence of the benzene ring stacking on to the CNT surface. In general, it is observed that the dispersive power of a surfactant is improved with the magnitude of the charge present on the surfactant molecule, the presence of benzene (or other saturated rings, such as naphthenic groups), or the presence of unsaturated carbon bonds (C=C) in the case of non-ionic surfactants such as Tween-20 or Tween-80. Moore, C.V. et al.[64] were among the first to perform a comparative study of the dispersion of SWNTs in various surfactants [Fig. 3(b)], including cetyltrimethylammonium bromide (CTAB), PEO–PPO–PEO triblock copolymer (Pluronic, various molecular weight sizes), Tween and Triton-X. For a comprehensive review of small molecule surfactants [Fig. 3(c)], the reader is referred to Vaisman, L. et al.[65]

2. Poly(ethylene glycol), PEG and its derivatives

PEG and its derivatives have long been used as a molecule of choice for functionalizing nanomaterials[66] for intracellular drug delivery[67] and targeted imaging.[68] This polymer is useful to render the nanomaterials biocompatible, increase their circulation lifetime *in vivo*, and to improve uptake and minimize clearance by the RES system,[69] i.e., "stealth" properties, because of its similarity to naturally-occurring carriers such as lipoproteins or viruses. Work done by Dai, H. and co-workers has adapted this method to be applicable to the dispersion of carbon nanotubes. One such approach uses a phospholipid-polyethylene glycol (PL-PEG) as a surface-coating agent for the non-covalent functionalization of SWNTs. PL-PEG is an amphiphilic polymer, in which the hydrophobic phospholipid chain sticks to the nanotube sidewall, while the hydrophilic PEG end faces outward, making a strong supramolecular complex
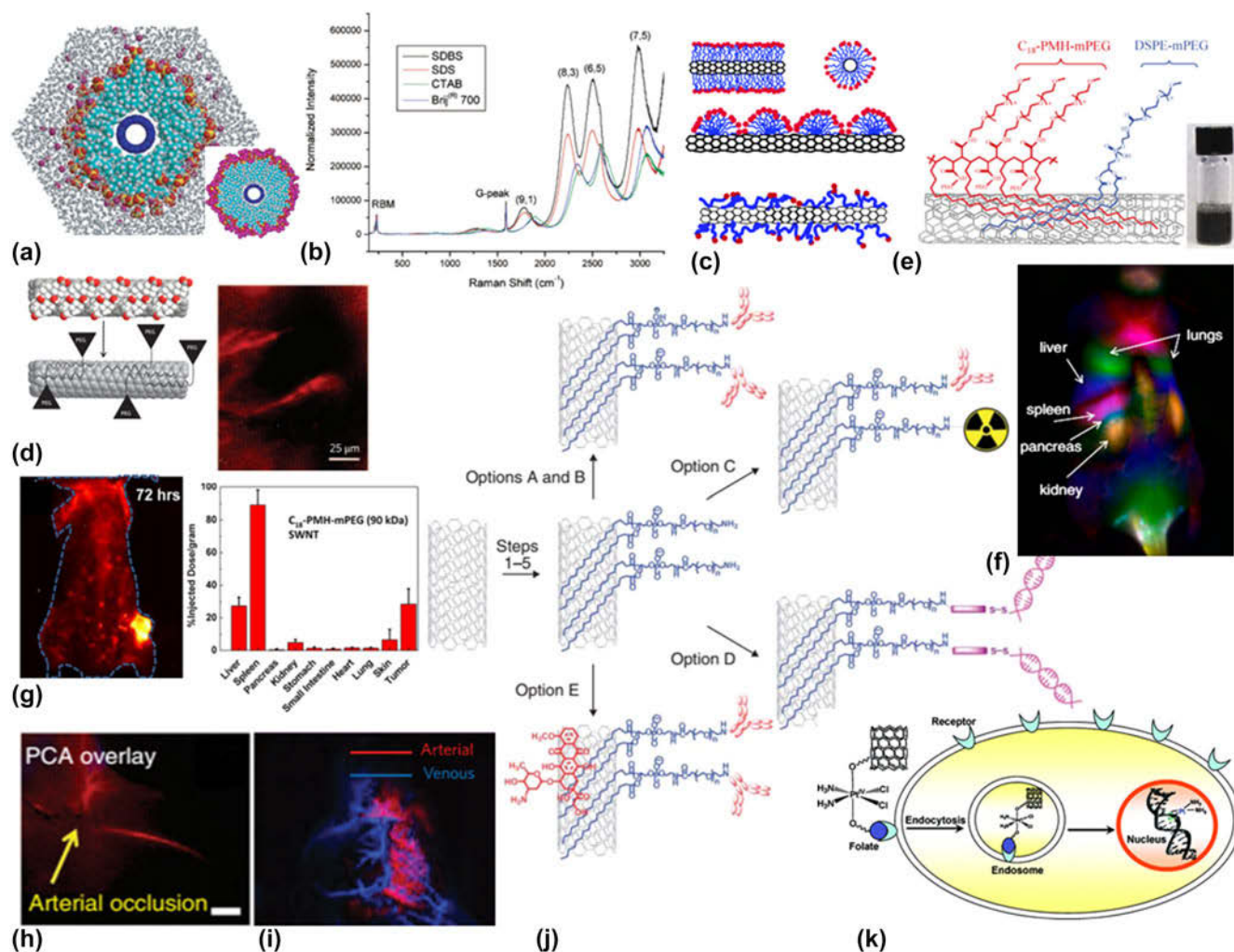
FIG. 3. Functionalization of SWNTs using small molecule surfactants and PEG derivatives. (a) MD simulation of water and SDS micelle around an SWNT, inset: an individual tube inside a cylindrical micelle. (b) Raman spectra of chirality-resolved SWNTs in various surfactants. (c) Mechanism of SWNT stabilization: cylindrical micelle, hemimicellar or random adsorption of surfactant molecules. (d) Surfactant exchange process, displacing cholate molecules with PL-PEG. This is used for intravital microscopy, with tumor vessel resolution ~microns. (e) Mixed (50–50%) C_{18}-PMH-mPEG and DSPE-mPEG surfactants to functionalize SWNTs. Inset shows photo of stable suspension. (f) PCA allows spatio-temporal resolution of anatomical organs, after injecting PEG-functionalized SWNT probes similar to (e). (g) Ultrahigh accumulation of C_{18}-PMG-mPEG-coated SWNTs in breast tumor xenograft (~30% injected dose/g), through the EPR effect. Clearance is mainly through the biliary pathway (feces). (h and i) Dynamic imaging of mouse vasculature, in a model of hindlimb ischemia (h) and cerebral artery occlusion (stroke) (i), using SWNTs similar to (e). (j) Protocols for the preparation of SWNT-based agents (options A, B: ligands, C: radiolabeling, D: siRNA, E: drug loading) for biomedical applications. (k) Example of targeted delivery of a Pt(IV) anticancer drug, using FA conjugated to SWNT-PL-PEG-NH$_2$. See text for definitions. Reprinted (adapted) with permissions from: (a) O'Connell et al.[63] © 2002 American Association for the Advancement of Science. (b, g, and k) Moore et al.,[64] Robinson et al.,[72] Dhar et al.[78] © 2003, 2012, 2008 American Chemical Society respectively. (c) Vaisman et al.[65] © 2006 Elsevier Publishing Group. (d, h, i, and j) Welsher et al.,[70] Hong et al.,[73] Hong et al.,[76] Liu et al.[80] © 2009, 2012, 2014, 2009 Nature Publishing Group, respectively. (e) Robinson et al.[156] © 2010 Springer. (f) Welsher et al.[71]

in water. One advantage of this functionalization technique is the ability to separate excess PL-PEG molecules from the solution by repeated centrifugation, as the method does not rely on micellar stabilization of SWNTs. In addition, the terminal –NH$_2$ or –COOH groups at the end of the PEG chain allow for the conjugation of targeting agents for specific applications. A drawback of this approach is that the extensive sonication used during the functionalization process

leads to significant sidewall damage, resulting in cutting of SWNTs into short segments, ~50–300 nm. This increases the defect density in the sidewall surface, and makes them less desirable for imaging applications. As an alternative, dialysis of the polymer from the reaction medium (post surface functionalization) can serve as an effective method to remove excess, unreacted PL-PEG.

In the first demonstration of the use of SWNTs as image contrast agents in mice, Welsher, K. et al.[70] used

a surfactant-exchange method, to displace the organic surfactant, sodium cholate, from the surface of SWNTs, with the PL-PEG polymer (1,2-distearoyl-*sn*-glycero-3-phosphoethanolamine-*N*-[methoxy(polyethyleneglycol)], 5 kDa mol wt). At an injected dose of 300 μL of ~170 μg/mL, they were able to perform high-resolution intravital microscopy imaging of tumor vasculature [Fig. 3(d)] beneath the skin. In further development, Welsher, K. et al.[71] have applied an image-processing technique called Principal Component Analysis (eigenvector decomposition) to track the whole-body blood circulation [Fig. 3(f)] of injected PL-PEG coated SWNTs. Using this time-resolved technique, coupled with the benefits of NIR-II imaging using SWNTs, they were able to distinguish organ-level anatomical features, by taking into consideration the hemodynamics of injected nanoparticles. Subsequently, Robinson, J.T. et al.[72] were able to obtain ultrahigh passive tumor uptake [Fig. 3(g)], ~30% injected dose/g (using enhanced permeability and retention, or the EPR effect) in a xenograft breast cancer model in mice, through long circulation lifetime (~20 h) of SWNTs solubilized using poly(maleic anhydride-*alt*-1-octadecene)-methoxy PEG, C18-PMH-mPEG. In parallel, Hong, G. et al.[73] have used DSPE-mPEG to stably suspend SWNTs in aqueous medium. Using these PEGylated SWNTs, they were able to visualize peripheral arterial disease in a mouse model [Fig. 3(h)], with high spatial (~30 μm) and temporal (<200 ms per frame) resolution, up to 3 mm depth, which offers ~3× improvement in spatial resolution compared to micro-CT imaging, without the drawbacks of long exposure (hours) and high radiation doses associated with the latter. It is worth noting here that these PEGylated SWNTs are useful for therapeutic applications, too, beyond the realm of non-invasive imaging. For example, Antaris, A.L. et al.[74] have demonstrated simultaneous tumor imaging and photothermal therapy (PTT), using chirality-separated (6, 5) SWNTs. Upon extension of the vascular imaging technique, Hong, G. et al.[75] have developed NIR-II fluorescence angiography, to track the regeneration of hind limb non-invasively, post ischemic surgery. Similarly, Hong, G. et al.[76] have demonstrated imaging at depths >2 mm in the mouse brain, through the skull, with sub-10 μm resolution. This method has the ability to dynamically observe blood perfusion in the cerebral vessels in real-time, and monitor blood flow during arterial occlusion in a model of cerebral stroke [Fig. 3(i)].

PEGylated carbon nanotubes have also been proven versatile as targeted drug-delivery systems. For example, Liu, Z. et al.[77] have shown ultrahigh loading capacity of doxorubicin, by π-stacking onto PEG-coated SWNTs, with pH-controlled release. Similarly, Dhar, S. et al.[78] have used amine-functionalized PEG-wrapped SWNTs to deliver folate-conjugated Pt(IV) complex, an anticancer drug [Fig. 3(k)], to selectively destroy FR$^+$ cells. In an *in*

vivo mouse model, Liu, Z. et al.[79] have shown ~10× tumor uptake of the water-insoluble drug, PTX, through the application of a SWNT–PTX conjugate, by loading the drug onto the branched PEG chains of the functionalized SWNT through a cleavable ester linkage. There is a wealth of available literature using different variants of this construct for targeted drug-delivery systems. For a thorough primer on the use of PL-PEG conjugation to prepare delivery vehicles (for radiolabels, drugs, image contrast agents, gene or siRNA delivery) based on SWNTs [Fig. 3(j)], the reader is referred to Liu, Z. et al.[80]

3. M13 bacteriophage

Work done in our research group, led by Belcher, A.M. and co-workers, has led to the development of M13 bacteriophage as a multifunctional platform, for synthesizing aqueous-dispersed, actively-targeted SWNTs [Fig. 4(a)], for non-invasively detecting, imaging and monitoring of cancers and infectious diseases in living hosts. M13 is a filamentous, non-lytic bacteriophage, with dimensions ~880 nm in length and ~6 nm in diameter. The five capsid proteins (p3, p5, p7, p8, and p9) of the virus can be genetically engineered to display peptides with multiple functionalities, such as targeting motifs against tumor cells (or against bacteria), drug molecules for therapy, or fluorescent probes for imaging. Specifically, our group has functionalized SWNTs longitudinally along M13, through a multivalent, high-copy π–π interaction. This M13-SWNT conjugate maintains sufficiently high fluorescence activity, in aqueous medium and upon *in vivo* injection into serum, to allow for high-quality NIR-II imaging of living subjects.

Yi, H. et al.[32] have demonstrated that the M13-functionalized SWNT probes can be detected in deep tissues, up to 2.5 cm in tissue-like phantoms, at very low dosage ~2 μg/mL. Further, using specific targeting of the prostate-specific membrane antigen (PSMA), they were able to show 4× improvement in uptake of the anti-PSMA-M13-SWNT probe, in a xenograft model of PSMA-positive prostate cancer [Fig. 4(a)]. In further development, Ghosh, D. et al.[33] have engineered the p3 protein to express a peptide against secreted protein, acidic and rich in cysteine (SPARC), which is overexpressed in aggressive subtypes of ovarian cancer. Using this targeting agent, the SPARC-binding peptide (SBP), the SBP-M13-SWNT probe was used in a pre-surgical planning of cytoreductive surgery in an orthotopic mouse model of human ovarian cancer. With a high target-to-background ratio ~112, they reported the detection of millimeter-scale tumors [Fig. 4(c)], which should improve "optimal debulking" upon clinical translation of this technology. Simultaneously, Bardhan, N.M. et al.[34] have shown the application of M13-SWNTs for fluorescence imaging of pathogenic infections; at an
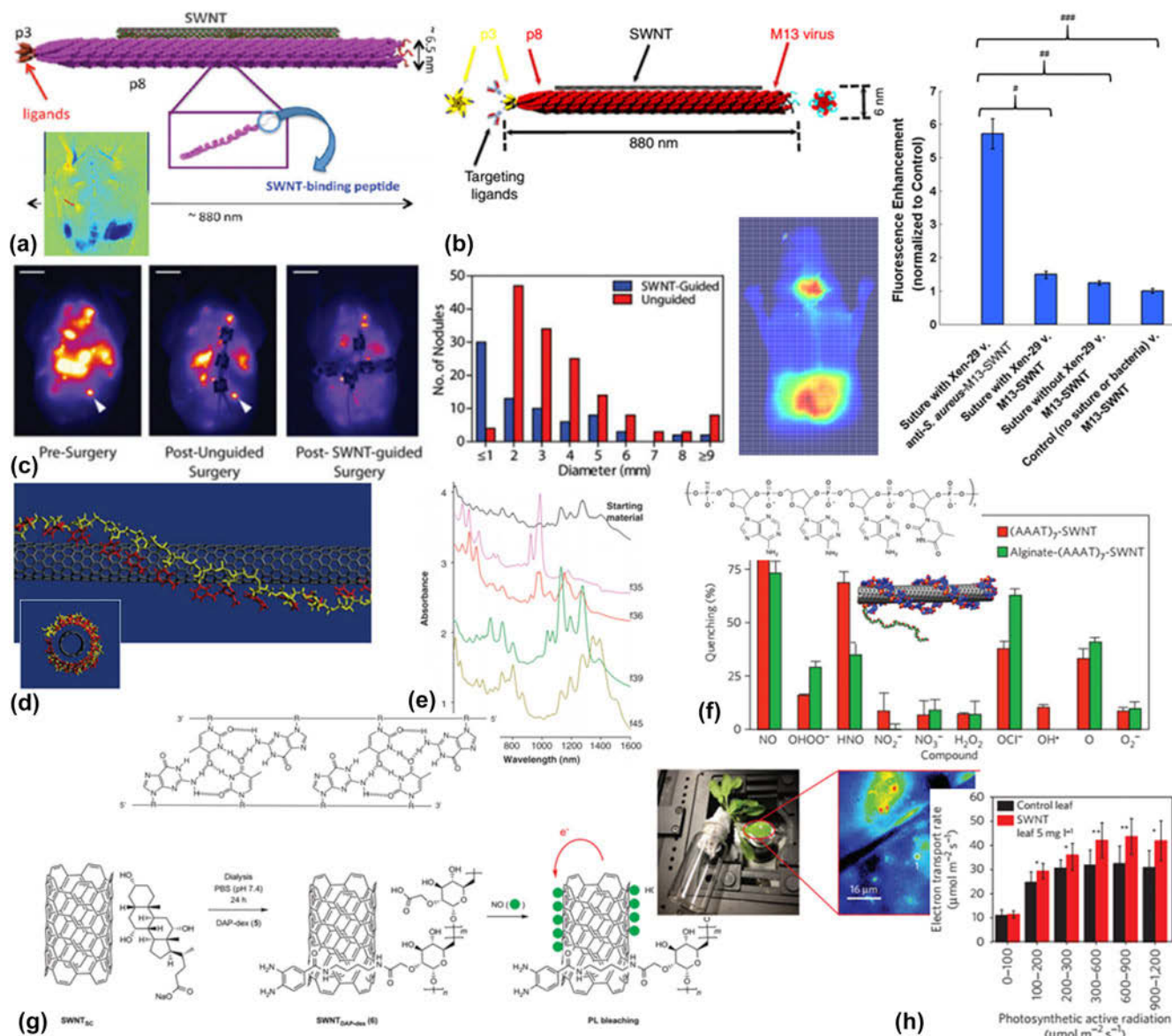
FIG. 4. Functionalization of SWNTs using M13 bacteriophage and DNA wrapping. (a) M13-functionalized SWNTs. Inset (bottom left) shows probe accumulation in a xenograft prostate tumor (red arrow), using anti-PSMA targeting. (b) M13-SWNT sensor used for detecting bacterial infections, targeted using antibodies labeled on the p3 end. Inset (bottom, center) shows deep-tissue imaging of an endocarditis model of *S. aureus* infection. Plot (right) shows fluorescence signal enhancement in the targeted case, relative to controls. (c) M13-SWNT probe used for pre-surgical planning, to improve surgical outcome in an orthotopic model of ovarian cancer. Plot (right) shows effectiveness of SWNT-guided procedure (blue bars) in removing a larger fraction of the smaller nodules ($\leq$1 mm size). (d) DNA-wrapped SWNTs. Binding model, with inset showing the "tube within a tube" structure making the SWNT water-soluble. (e) H-bonding interactions between 2 d(GT)$_n$ strands form a charge strip (inset, bottom left), which self-assembles around SWNTs depending on their chirality, and used for sorting the nanotubes (absorbance plot). (f) NO implantable inflammation sensor, based on quenching of the SWNT fluorescence. Inset (top left) shows the structure of the DNA oligonucleotide, ds(AAAT)$_7$ with selectivity to NO. (g) Synthesis of SWNT$_{DAP\text{-}dex}$ as a reversible sensor for NO detection. (h) "Plant nanobionics": infiltrating plant leaves with ss(AT)$_{15}$-SWNT leads to enhanced electron transfer, i.e., augmented photosynthesis. See text for definitions. Reprinted (adapted) with permissions from: (a) Yi et al.[32] © 2012 American Chemical Society. (b, d, f, g, and h) Bardhan et al.,[34] Zheng et al.,[81] Iverson et al.,[89] Kim et al.,[88] Giraldo et al.[92] © 2014, 2003, 2013, 2009, 2014 Nature Publishing Group, respectively. (c) Ghosh et al.[33] (e) Zheng et al.[82] © 2003 American Association for the Advancement of Science.

order-of-magnitude lower dosage compared to other small molecule organic dyes reported in the literature. In an intramuscular model of infection, the authors were able to obtain a ~3.4× enhancement in the fluorescence

signal intensity over background [Fig. 4(b)]. This was made possible by the use of NIR-II imaging with SWNTs, resulting in a lower signal spread, and higher signal amplification compared to shorter-wavelength

organic dyes. Further, in a mouse model of endocarditis (infection of the heart valves), they were able to image a ~5.7× enhancement in the signal intensity. This is an important milestone toward the non-invasive detection of deep-tissue infections, and could go a long way toward management of the problem of the spread of antibiotic-resistant infections in the clinic.

4. DNA wrapping

Several groups have reported the use of single-stranded DNA (ssDNA) for the functionalization of carbon nanotubes. The π–π interaction between the nanotube and the aromatic bases of ssDNA forms a functional complex, with the helical DNA structure extending along the length of the carbon nanotube. In this structure, the nitrogenous bases are attracted to the hydrophobic CNT structure, while the hydrophilic phosphate-sugar moieties face outward, making the complex water soluble, with low toxicity effects. In the first reported use of DNA wrapping, Zheng, M. et al.[81] showed helical wrapping of ssDNA on the surface of SWNTs, supported by molecular modeling [Fig. 4(d)]. Further, it was shown that it is possible to separate fractions of SWNTs based on their electronic structure [Fig. 4(e)], through DNA-wrapping, by chromatographic techniques. A significant advantage of using this method, compared to PEGylation or virus-templated functionalization, is the ability to select[82] and separate[83] the length[84] and chirality[85,86] of the SWNTs based on the sequence of DNA used. It has been shown to be systematically possible to individually sort all the major species of single-chirality SWNTs from a heterogeneous synthesized mixture, by using recognition sequences obtained from employing a randomized DNA library[87] with a diversity ~10^{60}.

Finally, it is worth mentioning a few other non-covalent approaches to SWNT functionalization, although they do not strictly fall into the above categories. Work done by Strano, M.S. and co-workers has focused on the detection of nitric oxide (NO) as a signaling molecule for inflammation. Kim, J-H. et al.[88] have designed an optical sensor [Fig. 4(g)] based on the detection of fluorescence modulation of SWNTs in the presence of NO, by wrapping the former with 3,4-diaminophenyl-functionalized dextran (DAP-dex), which only responds to NO but not to other reactive nitrogen or oxygen species. Subsequently, Iverson, N.M. et al.[89] have designed a double-stranded DNA oligonucleotide, ds(AAAT)$_7$, which allows for selectivity toward NO [Fig. 4(f)] and is used for wrapping the SWNT, which maintains its reactivity even after conjugation to 5 kDa PEG (for improving *in vivo* circulation). With a half-life of ~4 h, the sensor enabled detection of NO with a detection limit of 1 μM, with no immune

response to the implanted inflammation sensor observed over 400 days. This construct can also be used for the detection of intracellular signaling pathways through NO generation.[90] Using a similar approach, Iverson, N.M. et al.[91] have shown the detection of NIR-II fluorescence signal at ~5 mm depth in tissue, for alginate- or PEG-hydrogel-encapsulated ssDNA-wrapped SWNT nanosensors, in response to riboflavin. In yet another interesting manifestation, Giraldo, J.P. et al.[92] have come up with a "nanobionics" approach to augment photosynthesis [Fig. 4(h)], by suppressing the concentration of reactive oxygen species, and thereby increasing photosynthetic activity by ~3×, via the delivery of ss(AT)$_{15}$ DNA-coated SWNT–nanoceria composites in isolated chloroplasts through leaf infiltration.

B. Covalent functionalization of carbon nanotubes

The route to covalent functionalization involves a number of different chemical reaction approaches, each with their own benefits and drawbacks. While this Review aims to cover the main groups of reactions, it does not cover every possible reaction mechanism, and the reader is referred to an excellent review by Tasis, D. et al.[93]

1. Oxidation and hydrogenation reactions

The ability to perform "oxidative purification" of carbon nanotubes by liquid- or gas-phase oxidation is considered to be one of the milestones in nanotube chemistry.[94] This reaction leads to[95] the formation of defects in the sidewalls, cutting of the nanotube lengths, introduction of oxygen functional groups, and opening up of the end-caps[96] for closed nanotubes, along with the removal of metal catalysts that are present as impurities due to the nanotube synthesis process.[97] Oxidation of carbon nanotubes can be done using boiling HNO_3, H_2SO_4, "piranha" solutions (sulfuric acid with hydrogen peroxide),[98] or using combinations of ozone, air, or gaseous O_2 as oxidants at high-temperature, HF, OsO_4, H_2O_2, $K_2Cr_2O_7$, or $KMnO_4$, to name a few.[99]

In terms of applications, reaction-functionalized carbon nanotubes have long been eyed as efficient multifunctional vectors[100,101] for the delivery of therapeutics, gene delivery, as well as immunomodulatory probes. Chen, J. et al.[102] have designed biotin-functionalized oxidized SWNTs for receptor-mediated endocytosis and efficient delivery of taxoid molecules (a chemotherapeutic drug) into cancer cells [Fig. 5(d)]. Zhang, X. et al.[103] have used sodium alginate/chitosan-wrapped SWNTs after oxidative cutting, for loading and controlled release of doxorubicin to cancer cells [Fig. 5(c)], using folate targeting. Pescatori, M. et al.[104] have demonstrated that
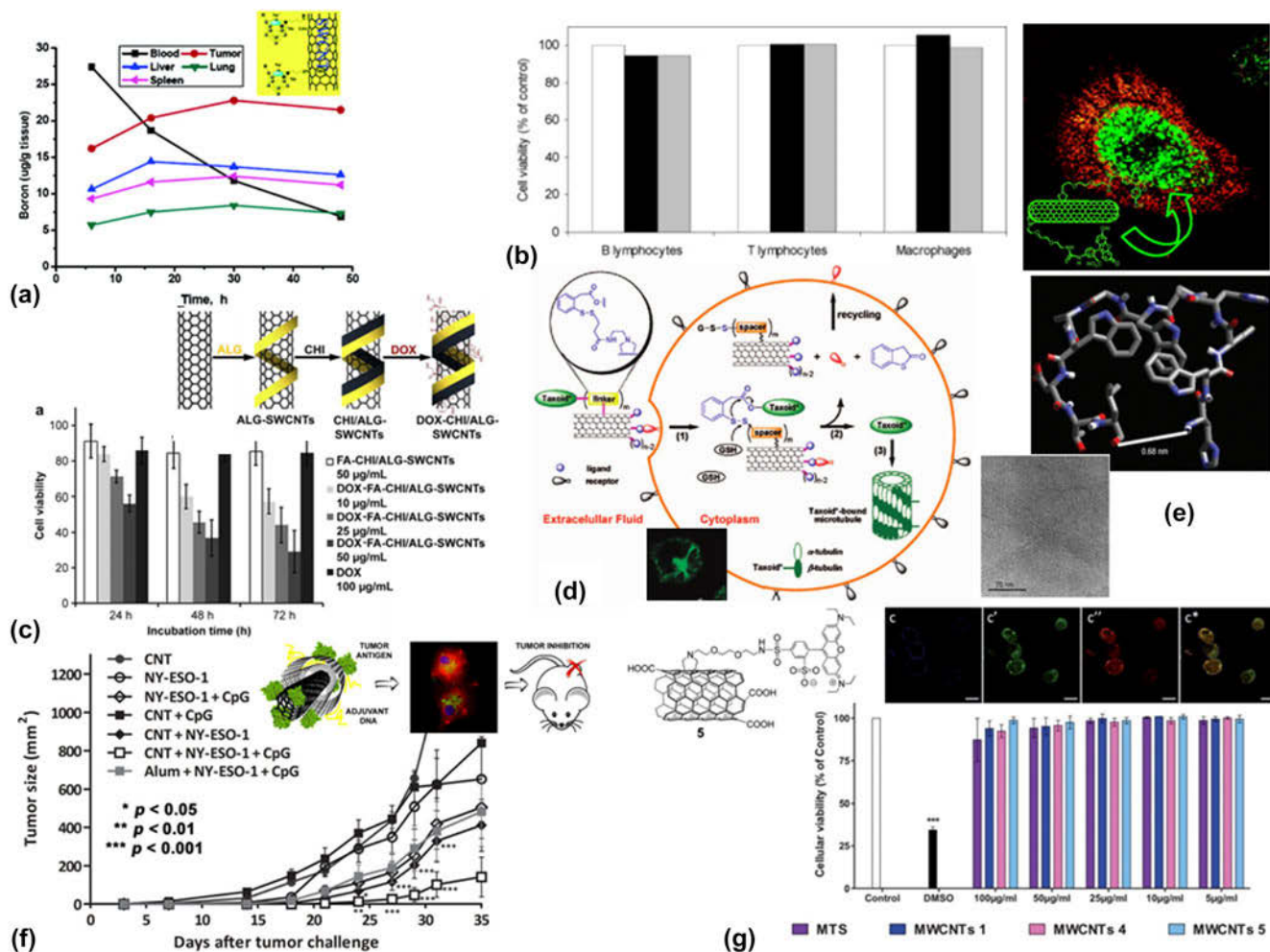
FIG. 5. Covalently functionalized SWNTs for biomedical applications. (a) Carborane (C_2B_{10}) cages attached to the sidewall of SWNTs (inset), and high boron uptake in EMT6 xenograft breast tumor; with potential application in boron neutron capture therapy. (b) Functionalized SWNTs through cycloaddition or through oxidation/amidation (inset) are non-cytotoxic to primary immune cells, at concentrations up to 50 μg/mL. (c) SWNTs functionalized with carboxylate groups, and wrapped with a polymer (alginate/chitosan) to load and deliver doxorubicin, targeted using FA, and drug release at pH 5.5. Plot shows viability of HeLa cells, with enhanced cytotoxicity compared to free drug. (d) A rationally designed drug delivery vehicle, based on SWNTs, using receptor-mediated endocytosis. Inset (bottom left): Microtubule networks in L1210 murine leukemia cells, generated by cleavage of the S–S bond in the linker by intracellular thiol. (e) Phage-display to identify peptides with binding affinity to SWNTs. Example of a low-energy conformation of a binding sequence, rich in histidine (H) and tryptophan (W). Inset: TEM shows bundling of CNTs, caused by loss in functionalization capability due to a point mutation of W to S (serine). (f) CNTs for vaccine delivery. Inset: Oxidized MWNTs used to deliver CD^{8+} T-cell promoter antigens, as an anticancer vaccine. Plot shows delay in tumor growth in dosed mice challenged with the B16F10 transgenic melanoma cell line, and showed prolonged survival (not shown here). (g) Mitochondrial targeting sequence (MTS) peptides used to deliver CANOMATs into organelles inside HeLa cells. Inset (top left): MTS-MWNT, (top right): confocal images, showing colocalization of CNT (red) into the mitochondria (yellow). Reprinted (adapted) with permissions from: (a, b, d, and f) Yinghuai et al.,[157] Dumortier et al.,[158] Chen et al.,[102] de Faria et al.[105] © 2005, 2006, 2008, 2014 American Chemical Society, respectively. (c) Zhang et al.[103] © 2009 Elsevier Publishing Group. (e) Wang et al.[113] © 2003 Nature Publishing Group. (g) Battigelli et al.[117] © 2013 Royal Society of Chemistry.

oxidized nanotubes act as cell-specific immunostimulatory systems, as they were observed to activate immune-related pathways in monocytes but not in T-cells, associated with inflammatory processes occurring during immune-mediated tumor rejection and pathogen clearance. de Faria, P.C.B. et al.[105] have used oxidized multiwall nanotubes as an anticancer vaccine formulation, with rapid internalization into dendritic cells, both *in vitro* and *in vivo*. This

resulted in strong responses against the antigen, by $CD4^+$ and $CD8^+$ T-cells, and the vaccination was reported to significantly delay tumor development [Fig. 5(f)] and prolong the survival of the mice used in the study. In a recent report, Fedeli, S. et al.[106] have synthesized oxidized MWNTs loaded with doxorubicin, showing enhanced cytotoxic effect in MCF-7 breast cancer-induced mice, compared to the free drug.

2. Polymer conjugation

Broadly speaking, there are two main approaches[107] to covalent functionalization by polymerization: "grafting to" and "grafting from". The former approach has been very well explored, through reactions such as amidization[108] and esterification.[109] In contrast, the latter has been used to graft polymer chains onto solid substrates, starting from polymer-functionalized carbon nanotubes. For example, Viswanathan, G. et al.[110] have developed a method to in situ composite synthesis, by conjugating polystyrene (PS) chains to full-length pristine SWNTs, without disrupting the original structure, by using an anionic polymerization scheme. Qin, S. et al.[111,112] have reported the grafting of n-butyl methacrylate and PS, to form "polymer brushes" from SWNTs, by atom-transfer radical polymerization, which could theoretically be applied to a wide range of vinyl polymers. It was claimed that initiator functionalization and polymerization did not change the sidewall structures of the SWNT significantly, according to Raman and near-IR spectra measurements.

Finally, as a class of biological polymers, several groups of researchers have demonstrated SWNTs functionalized with peptides[113–115] [Fig. 5(e)], which can be designed to retain their biological function, such as immunogenicity, and can be used to elicit an antibody response with the right specificity. These approaches can be greatly suitable for in vivo diagnostic and therapeutic purposes, such as vaccine[116] and gene delivery[117,118] systems, as well as an exciton quenching-based optical sensing for single-molecule detection of nitroaromatic compounds.[119]

IV. FUNCTIONALIZATION OF GRAPHENE

A summary of the various techniques of functionalization used for graphene and its derivatives is presented in Table 3 in the Supplementary Material.

A. Non-covalent functionalization of graphene and its derivatives

Since pristine graphene sheets are hydrophobic in nature, they cannot be dissolved in polar solvents. This makes it important to functionalize them for biomedical applications. Similar to carbon nanotubes, the functionalization by π-interactions is a beneficial approach, since it can enable the attachment of functional groups to graphene without changing the long-range electronic network of sp^2-bonded carbon, while introducing additional selective properties to graphene and its derivatives.

1. DNA functionalization

The use of DNA as a self-assembly template has proven to be an attractive route to synthesize structures into well-defined 1- or 2-dimensional arrays, or other unique geometries through techniques such as "DNA Origami".[120] For example, Mohanty, N. and Berry, V.[121] have demonstrated a suite of bioelectronics technologies [such as a single-bacterium resolution interfacial device, a label-free, reversible DNA detector, and a polarity-specific molecular transistor for DNA adsorption, Fig. 6(a)] at the microbial and molecular levels, using chemically-modified graphene. Patil, A.J. et al.[122] have reported the use of ssDNA to stably disperse single-layer graphene in aqueous suspensions, at concentrations as high as ~2.5 mg/mL [Fig. 6(e)]. Simultaneously, Liu, J. et al.[123] developed a method to decorate GO and reduced GO (rGO) with DNA, and used it to pattern Au nanoparticles into two-dimensional arrays [Fig. 6(c)]. This approach has the benefit of good stoichiometric control over the ratio of nanoparticles to the graphene nanosheets, compared to other in situ growth methods. In parallel, Lu, C-H. et al.[124] have shown the application of GO as a platform for fast, sensitive detection of biomolecules such as DNA, by restoration of the fluorescence emission [Fig. 6(b)] through a binding event of a complementary sequence of DNA (analyte to be detected) to the one with quenched signal adsorbed on the surface of GO. Later, Xu, Y. et al.[125] have reported a facile 3D self-assembly method to prepare GO/DNA composite hydrogels [Fig. 6(d)], with high mechanical strength, high dye-loading capacity, good environmental stability, and self-healing capability. These mechanically flexible, electrically conductive, functionalized graphene substrates offer new opportunities for bio-nanodevices.

2. Poly(ethylene glycol)

The method of PEGylation of GO and rGO has long been investigated, for the purposes of cell imaging and drug delivery. A detailed analysis by Wojtoniszak, M. et al.[126] reveals that such functionalization promotes biocompatibility of GO and rGO, over a wide range of concentrations, ~25–3125 μg/mL, with low cytotoxicity effects [Fig. 7(c)]. These considerations are important while designing graphene-based nanocarriers for in vivo theranostic applications. As an example, Robinson, J.T. et al.[127] developed nanosized rGO, ~20 nm in size, with non-covalently functionalized PEG, with an Arg-Gly-Asp (RGD) targeting motif for highly effective photoablation of cells in vitro. In the field of biosensor device applications, Yoon, H.J. et al.[128] have non-covalently functionalized GO with PL-PEG-NH$_2$, and used this construct to decorate EpCAM antibodies [Fig. 7(e)] for the capture of circulating tumor cells with a capture yield of ~73% in whole blood [Fig. 7(f)]. Building on this approach, the same group of researchers have developed[129] functionalized GO dispersed in a matrix of thermoresponsive polymer for thermally-triggered release of the cells post-capture. In a recent report, Gupta, B. et al.[130]
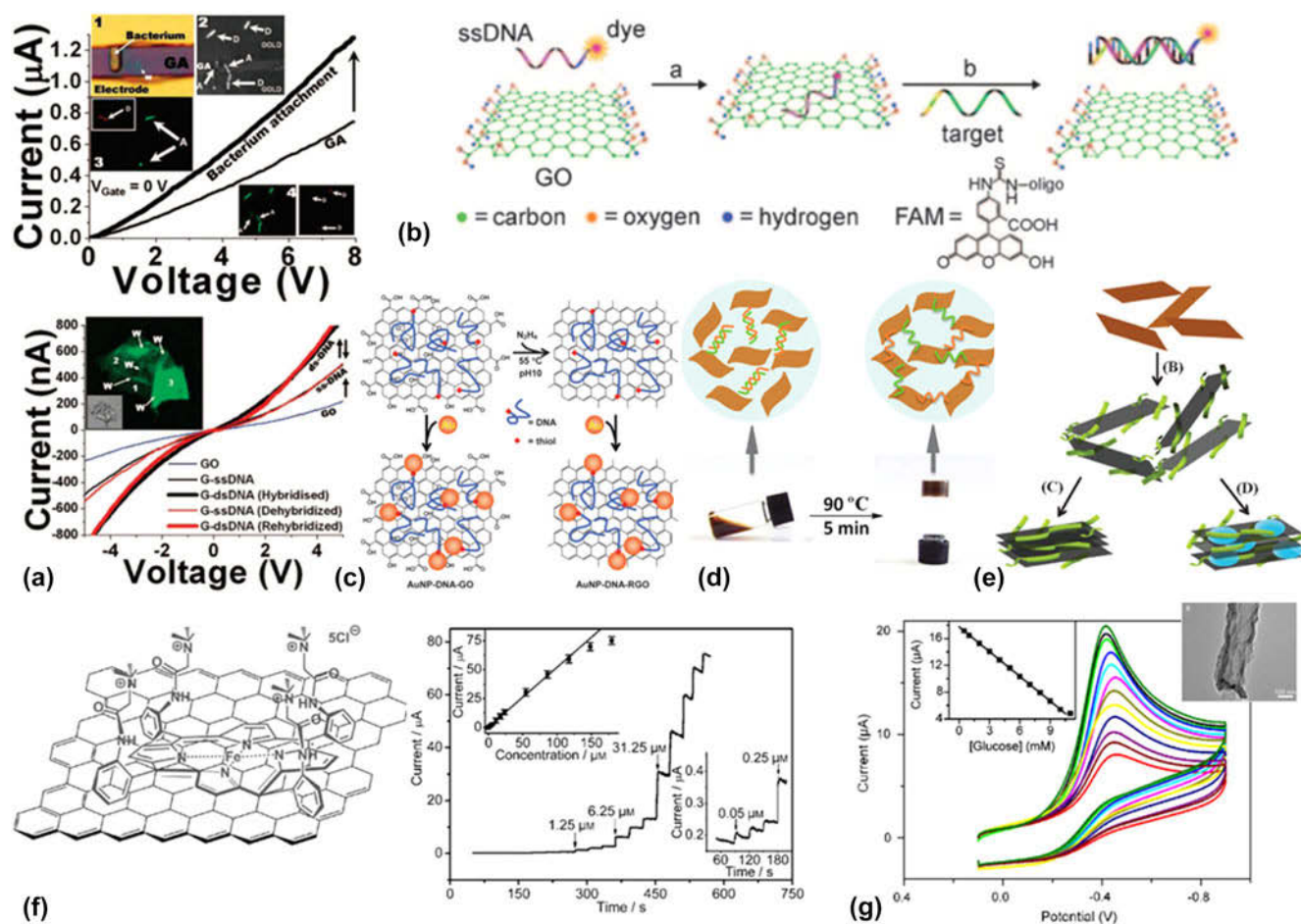
FIG. 6. DNA- and porphyrin-functionalized graphene. (a) (left) Single cell bacterial attachment, through electrostatic deposition on the graphene-amine substrate, and (right) DNA transistor: ss-DNA tethering increases the conductivity of the GO-based device. (b) Biosensor based on target-induced fluorescence change of the fluorescein-based dye, used for fast, sensitive detection. (c) DNA coating resulting in aqueous dispersion of GO and rGO, which were then used to form a 2D "bionanointerface" for an assembly of Au-carbon heterostructures. (d) GO/DNA self-assembled hydrogel, with high dye adsorption capacity, environmental stability, and self-healing capability. (e) DNA-stabilized aqueous suspensions of graphene, used to synthesize ordered, lamellar multifunctional nanocomposites for biosensing. (f) Noncovalent assembly of FeTMAPP on rGO, and its amperometric response to successive concentrations of chlorite biosensing, which can have applications for drinking water monitoring after disinfection by bleach. (g) Cyclic voltammetry curves showing the response of an amperometric biosensor for glucose detection, through glucose oxidase-catalyzed reduction of oxygen, using porphyrin-functionalized reduced graphene nanoribbons. Inset shows TEM image of the GO nanoribbons. See text for definitions of molecules. Reprinted (adapted) with permissions from: (a and d) Mohanty and Berry,[121] Xu et al.[125] © 2008, 2010 American Chemical Society respectively. (b, e, and f) Lu, C-H. et al.,[124] Patil et al.,[122] Tu et al.[159] © 2009, 2009, 2010 John Wiley and Sons, respectively. (c) Liu et al.[123] © 2009 Royal Society of Chemistry. (g) Zhang et al.[160] © 2011 Elsevier Publishing Group.

have reported a facile, chemically clean, and environmentally green method to modify the oxygen functionalization and intercalate PEG200 within rGO, through the use of hydrogen-bonding [Fig. 7(g)]. This method preserves the chemical and structural integrity of the carbon network in rGO, and also provides an effective dispersion of the hydrophilic polymer in the rGO, which is useful as a lubricating agent. The thin film was demonstrated to have application as a solid-state lubricant, with improved wear resistance to γ-irradiation. While there have been no reports yet of biomedical applications of this technique, it may find use in providing lubrication coatings for implants and prosthetic joints.

3. Other approaches to functionalization

While the above sections listed the most common techniques for the non-covalent functionalization of graphene and its derivatives, there are numerous examples of unconventional methods used in the literature.

Work done in our group, in collaboration with Grossman, J.C. and co-workers, has led to the development of a 1-step, mild thermal annealing process at
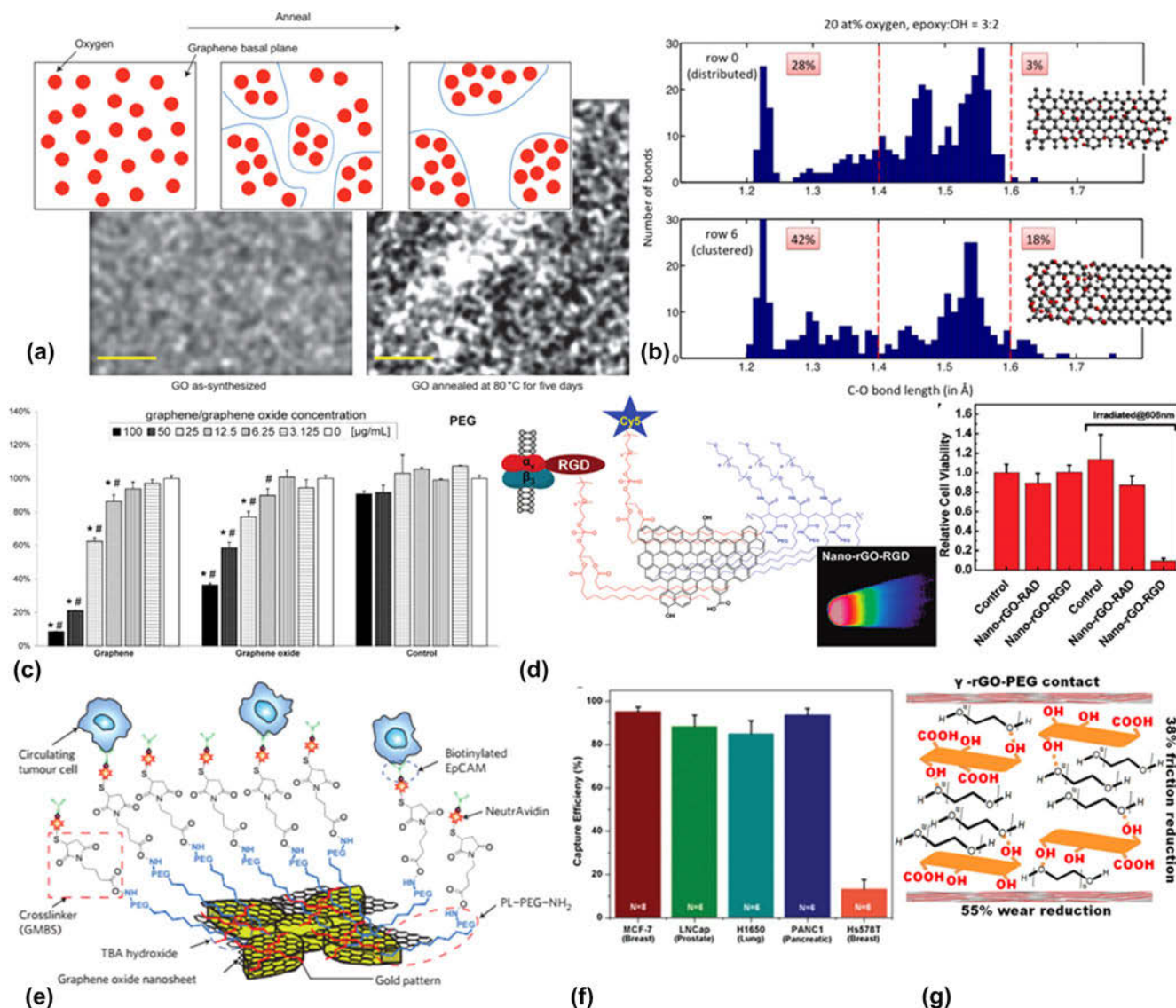
FIG. 7. Other approaches to PEGylation and non-covalent functionalization of graphene. (a) Schematic showing the phase transformation process, causing redistribution of the mixed sp^2–sp^3 phases into distinct oxidized and graphitic domains, effected by mild thermal annealing of GO at T = 80 °C. Red circles indicate oxygen functional groups. Inset: Auger-electron spectrographs taken on SEM images show distinct oxygen-rich regions (white) separated by channels of graphene (black). (b) MD simulations show changes in the carbon-oxygen bonding environment in GO, caused by thermal annealing. Due to oxygen clustering, a greater fraction of the carbon–oxygen bonds form carbonyls (C=O), with weaker bond strengths and greater reactivity to nucleophilic attack. (c) Cell viability assay on L929 fibroblasts, treated with PEGylated graphene and GO, showing good cytocompatibility up to ~12.5 μg/mL. The PEG is non-covalently adsorbed on the graphene basal plane. (d) PTT achieved using a nano-GO-RGD construct (inset), showing highest heating capability. Plot shows relative viability of U87MG human glioblastoma cells, with maximum therapeutic effect observed in RGD-targeted PTT. (e) Structure of GO adsorbed on patterned gold, and subsequently functionalized with EpCAM antibodies for isolating circulating tumor cells from whole blood. (f) Efficient capture and release of CTCs using a polymer–GO composite. (g) Non-covalent PEGylation of rGO by γ-radiolysis, resulting in an effective dispersion with lubrication properties. See text for definitions of molecules. Reprinted (adapted) with permissions from: (a and e) Kumar et al.,[131] Yoon et al.[128] © 2014, 2013 Nature Publishing Group, respectively. (b and c) Kumar et al.,[132] Wojtoniszak et al.[126] © 2016, 2012 Elsevier Publishing Group, respectively. (d and g) Robinson et al.,[127] Gupta et al.[130] © 2011, 2016 American Chemical Society, respectively. (g) Yoon et al.[129] © 2016 John Wiley and Sons.

80 °C, to improve the properties of as-synthesized GO[131] and rGO.[132] This approach is unique because it relies simply on the thermal annealing treatment, with no additional chemical modifications involved. Moreover, it is scalable, and can be applied to a wide variety of samples in the form of suspensions, powders, thin films,

and free-standing GO paper. The method works by promoting a redistribution of the oxygen functional groups on the graphene basal plane, through a phase transformation process, which drives the diffusion of the oxygen functional groups from the inhomogeneous, randomly-distributed, mixed sp^2–sp^3 state into distinct

oxidized (sp^3) and graphitic (sp^2) domains [Figs. 7(a) and 7(b)], while preserving the total oxygen content of the system. Consequently, this annealing treatment results in an improvement in the sheet resistance of as-synthesized GO by 4 orders-of-magnitude, an improvement in the visible absorption by up to 38%, and a tunable, controlled blue-shift in the photoluminescence spectrum, which can be exploited in the fabrication of biosensing devices. This method is used for enhancing the cell capture efficiency of white blood cells from whole blood, as described in Sec. IV. B. 1.

B. Covalent functionalization of graphene and its derivatives

There have been several procedures developed to attach chemical functionalities to graphene—either through direct reaction with pristine graphene sheets, or through chemical modification of GO or rGO.

1. Poly(ethylene glycol) and other polymers

GO has been grafted with polymer chains containing reactive functional groups such as hydroxyls and amines. Different polymers have been used for this purpose, including PEG, polylysine, polyallylamine, poly(vinyl alcohol), and PS, to name a few. For example, Liu, Z. et al.[133] have developed PEGylated nanographene oxide in water, and used it to non-covalently load a water-insoluble anti-cancer drug molecule, SN38, through π–π stacking. This construct was found to be ~1000× more potent than a clinically approved camptothecin prodrug molecule; almost comparable to free drug in DMSO [Fig. 8(a)]. Using a similar approach on pristine graphene nanosheets, Yang, K. et al.[134] showed highly efficient passive targeting (via the EPR effect) in xenograft tumors in mice. Subsequent near-infrared PTT showed an improvement in survival from ~16 days (untreated control) to >40 days with the treatment [Fig. 8(b)]. Building upon this approach, Zhang, W. et al.[135] have used NIR PTT in synergy with chemotherapy (doxorubicin) loaded onto PEGylated nano-GO, for achieving higher therapeutic efficacy, in a xenograft mouse model. Tian, B. et al.[136] have attempted to use photodynamic therapy (PDT) enhanced by PTT, by loading a photosensitizer molecule (Chlorin e6) onto PEG–GO [Fig. 8(c)]. As a follow up to this approach, Cao, J. et al.[137] have used diffusion-weighted MRI to monitor the effectiveness of PTT/PDT [Fig. 8(d)], with the most effective treatment resulting in tumor-free condition after 60 days. Similarly, Feng, L. et al.[138] have used dual polymer-functionalized nano-GO (PEG and polyethyleneimine, PEI) to achieve light-controlled delivery of siRNA, by increasing the cell membrane permeability using low-power NIR irradiation. In an alternative approach, Shan, C. et al.[139] have covalently functionalized water-soluble graphene using biocompatible poly(L-lysine), PLL. PLL is an attractive polymer functionalization agent, which has applications such as biosensing, promoting cell adhesion, drug delivery, and electrochemical sensing. By immobilizing horseradish peroxidase on the PLL–graphene nanocomposites, they demonstrated amplified biosensing of H_2O_2. Similarly, Hu, S-H. et al.[140] have attached quantum dots on PLL-coated rGO, for folate-targeted cellular imaging and *in situ*-monitored PTT. Hong, H. et al.[141] have used ^{64}Cu-labeled PEGylated GO, for in vivo PET imaging of subcutaneous xenograft tumors [Fig. 8(e)] through active targeting of the tumor neovasculature using CD105 overexpressed in many solid tumors. For an excellent primer on the protocol for the functionalization of graphene and its derivatives with PEG, the reader is referred to Yang, K. et al.[142]

Work done in our own research group, in collaboration with Ploegh, H.L. and co-workers, has made good use of the functionality afforded by PEG-conjugated GO. GO was functionalized with diamine-terminated PEG (NH_2–$(PEG)_n$–NH_2). The terminal amines of the PEG chains were then reacted with dibenzocyclooctyne-*N*-hydroxysuccinimyl ester (DBCO-NHS), to activate it for a "click" coupling reaction. We then conjugated VHH7 nanobodies (single-chain only fragments of conventional antibodies, which are specific to murine Class-II MHC$^+$ cells) to the DBCO handle. Using this chemistry, we were able to show highly efficient, very specific cell capture[35] of white blood cell populations from small volumes (~30 μL) of murine whole blood [Fig. 8(g)], using a relatively inexpensive device (without the need for cell sorting or microfluidic apparatus), under ambient conditions.

2. Free radical addition

Organic free radicals and dienophiles with affinity toward the C=C sp^2 carbons in graphene are some of the most attractive candidates for reactive covalent functionalization of graphene. For example, the reaction of a diazonium salt,[143] or other reducing agents such as hydrazine monohydrate (N_2H_4·H_2O)[144] with the unsaturated carbons results in the formation of nitrophenyls on the graphene sheet. Such covalent functionalization results in the introduction of a band gap (~0.4 eV)[145] in the normally zero-gap pristine graphene, which makes it a suitable candidate for semiconducting applications. Several other groups of researchers, such as Sharma, R. et al.[146] and Hossain, M.Z. et al.[147] have demonstrated high reactivity of graphene sheets toward nitrophenyl-contributing electron acceptor diazonium salts. Alternatively, Liu, H. et al.[148] have shown free radical addition of phenyl groups, by photo-activated initiator reaction of benzoyl peroxide in toluene,
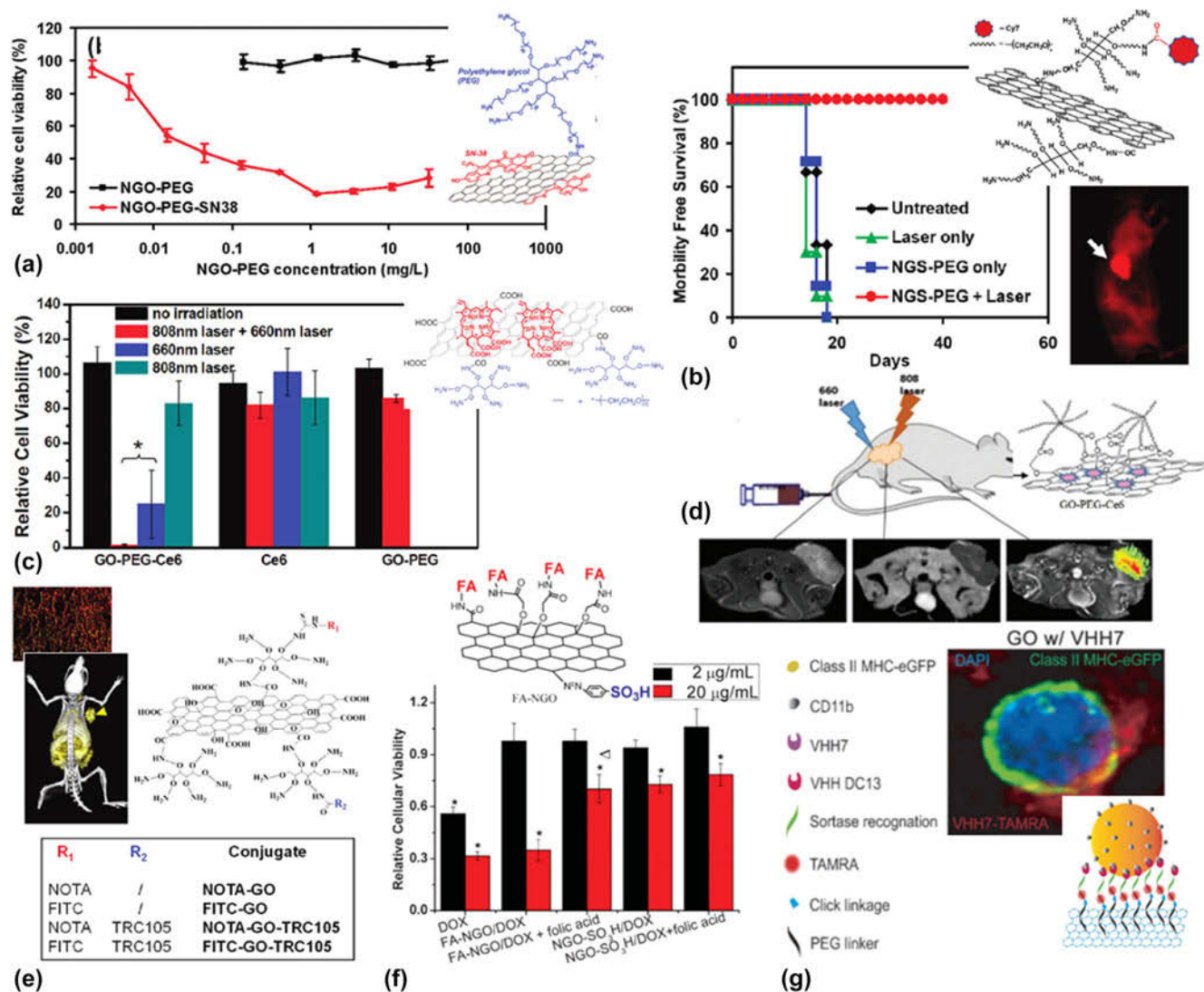
FIG. 8. Covalent functionalization of PEG and other moieties to graphene. (a) PEGylated nano-GO complex loaded with SN38 drug analog, shows high toxicity to human colon cancer cells, HT-116 *in vitro*. Inset shows the structure of the complex. (b) Ultrahigh tumor uptake of PEG-functionalized nanographene sheets (white arrow, inset). PTT at 2 W/cm^2 leads to survival of the entire group of subjects (up to 40 days). (c) Photothermally enhanced delivery of PDT using PEGylated GO, at a conc. of 2.5 μM Ce6 (photosensitizer), with the best effect obtained in the synergistic case (red bars). Inset shows the structure of the GO-PEG-Ce6 molecule. (d) Diffusion-weighted MRI can be used to monitor the efficacy of the PTT/PDT combination therapy, with the same molecule as in (c). (e) *In vivo* PET imaging of 4T1 murine breast tumor (indicated by arrow), using ^{64}Cu-labeled PEGylated GO (structure shown to the right). (f) *In vitro* assay of cell viability ($t = 48$ h) on MCF-7 breast cancer cells, using FA-targeted nano-GO, loaded with mixed drugs (doxorubicin and camptothecin). PEG-functionalized GO shows very little toxicity, while loading with drug cocktail reduces cell viability. (g) Cell capture assay based on VHH7 "nanobodies" (single-domain antibodies) decorated on PEGylated GO substrate. Inset: confocal image of Class-II MHC$^+$ cell, captured from whole blood. See text for definitions of molecules. Reprinted (adapted) with permissions from: (a, b, c, and e) Liu et al.,[133] Yang et al.,[134] Tian et al.,[136] Hong et al.[141] © 2008, 2010, 2011, 2012 American Chemical Society, respectively. (d) Cao et al.[137] © 2016 Royal Society of Chemistry. (f and g) Zhang et al.,[149] Chen et al.[35] © 2010, 2015 John Wiley and Sons, respectively.

resulting in the attachment of the benzene ring through an sp^3 bond on to the graphene substrate.

In terms of applications, the availability of a rich chemistry of functional agents lends itself to creative uses in biology and medicine. For example, Zhang, L. et al.[149] used sulfonation with the aryl diazonium salt of sulfanilic acid, to introduce SO$_3$H groups, and then conjugate folic acid (FA) onto nano-GO. Through controlled loading of

2 anticancer drugs, doxorubicin and camptothecin, via π–π stacking, they reported much higher cytotoxicity against MCF-7 breast cancer cells compared to the activity of each drug used individually [Fig. 8(f)]. Zhang, X. et al.[150] have developed hybrid materials of graphene with porphyrin, namely, graphene–tetraphenylporphyrin (graphene–TPP) and graphene–palladium tetraphenylporphyrin (graphene-PdTPP)

through a one-pot cycloaddition synthesis route, with potential applications in fluorescence imaging of cells and in sensors. Wei, G. et al.[151] have used a wet-chemical diazotization method, to functionalize rGO with *p*-aminobenzoic acid. After the introduction of PEI and target molecule FA, they were able to load and deliver elsinochrome A (EA) and doxorubicin, which showed synergistic effect of enhanced chemotherapeutic efficacy by arresting cell cycle activity in the G2 phase. In another work, Gollavelli, G. and Ling, Y-C.[152] have designed multi-functional graphene with magnetic, water-solubility and fluorescence properties, by covalently attaching poly(acrylic acid), PAA and fluorescein *o*-methacrylate on rGO, using benzoyl peroxide activated by microwave irradiation. Using this approach, they were able to perform *in vitro* cellular imaging in HeLa cells, and *in vivo* in zebrafish. For a good review on the use of chemically modified graphene in synthetic biology, the reader is referred to Servant, A. et al.[153]

V. CONCLUDING REMARKS AND FUTURE DIRECTIONS

In this Review, we have undertaken a landmark survey of the progress made in the past 30 years, with respect to the functionalization of CANOMATs for biomedical applications. This investigation has been done taking into account relevant considerations such as the method of functionalization, the number of steps, and time required, need for special equipment, the phases in which the method can work, the properties affected, techniques to characterize the product, and importantly, whether the approach is robust enough to be scalable and reproducible, with a list of the applications explored till date. The rapid advances in the methods of functionalization, with consequent applications in targeting, imaging, and drug delivery (in pre-clinical models), have been nothing short of breathtaking.

That being said, it seems a bit disappointing, though hardly surprising, to note that very few (if any?) of these novel materials have actually made it past the research laboratory to clinical practice (i.e., from the "bench" to the "bedside"). Why is this so? Part of the reason is the regulatory burden of proving safety and efficacy of these materials prior to being approved for diagnostic or therapeutic use (for a brief discussion on the safety of CANOMATs in living organisms, refer to Sec. 5 of the Supplementary Material). However, the author opines that a bigger factor is the lack of a systematic plan to identify the areas where the applications of CANOMATs would have the most impact in human medicine. Toward this end, here are a few recommendations to direct our collective efforts in materials research, for making them more suitable for clinical translation:

(1) Test safety and efficacy in larger animal models: almost all the proof-of-principle studies of targeting, as well as long-term biodistribution studies of the safety of CANOMATs, have relied on rodent models (mice or rats). As a step toward first-in-human testing, these materials need to be tested for safety in larger animals; perhaps in porcine models, and then in primates.

(2) Build an adaptive, hierarchical nano-scale architecture: there is a need for adaptive materials design, to be reversibly scalable, on-demand, *in vivo*, from the nano-scale to the bulk: through processes such as self-assembly or bond cleavage, mediated by environmental factors such as pH-, oxygen content-, temperature-, or light-activation for smart applications.

(3) Implement composites of C_{60}-SWNT-GO: composite CANOMATs can provide a synergistic advantage by augmenting their complementary properties. For example, it may be possible to design large-area biosensors based on functionalized GO, which use SWNTs for an optical readout, and C_{60} derivatives to encapsulate and deliver drug molecules, while avoiding the limitations posed by each of these individual nanomaterials.

(4) Integrate bio-nano-composites: there is a pressing need to undertake research based on the idea of "convergence", which aims to refine our nanotechnology toolkits by understanding the behavior of materials at the interface of engineering and biology. This is increasingly important as we aim to transition toward a "personalized medicine" approach in cancer therapy.

(5) Design molecular probes to penetrate the blood–brain barrier: the efficacy of nanotechnology-based approaches toward the treatment of brain tumors, cerebral stroke, and other neurological disorders such as Alzheimer's or Parkinson's has been limited,[154] due to problems with overcoming the BBB. More rational design choices need to be considered, to make CANOMATs the preferred mode of drug delivery by overcoming the physiological barriers of the brain.

The question that medical professionals in the clinic should be asking, is: "Can we CANOMAT?" the answer, with cautious optimism, is "Yes, we can."

122

J. Mater. Res., Vol. 32, No. 1, Jan 13, 2017

REFERENCES

1. H.W. Kroto, J.R. Heath, S.C. O'Brien, R.F. Curl, and R.E. Smalley: C_{60}: Buckminsterfullerene. *Nature* **318**(6042), 162 (1985).
2. S. Iijima: Helical microtubules of graphitic carbon. *Nature* **354**(6348), 56 (1991).
3. K.S. Novoselov, A.K. Geim, S.V. Morozov, D. Jiang, Y. Zhang, S.V. Dubonos, I.V. Grigorieva, and A.A. Firsov: Electric field effect in atomically thin carbon films. *Science* **306**(5696), 666 (2004).
4. M.S. Dresselhaus, G. Dresselhaus, and P.C. Eklund: *Science of fullerenes and carbon nanotubes* (Academic Press, San Diego, 1996).
5. R. Saito, G. Dresselhaus, and M.S. Dresselhaus: *Physical properties of carbon nanotubes* (Imperial College Press, London, 1998).
6. H. Dai: Carbon Nanotubes: synthesis, integration, and properties. *Acc. Chem. Res.* **35**(12), 1035 (2002).
7. A.K. Geim and K.S. Novoselov: The rise of graphene. *Nat. Mater.* **6**(3), 183 (2007).
8. Z. Liu, S. Tabakman, K. Welsher, and H. Dai: Carbon nanotubes in biology and medicine: *In vitro* and *in vivo* detection, imaging and drug delivery. *Nano Res.* **2**, 85 (2010).
9. R. Bakry, R.M. Vallant, M. Najam-ul-Haq, M. Rainer, Z. Szabo, C.W. Huck, and G.K. Bonn: Medicinal applications of fullerenes. *Int. J. Nanomed.* **2**(4), 639 (2007).
10. J. Conyers and P. Ranga: Biomedical applications of functionalized fullerene-based nanomaterials. *Int. J. Nanomed.* **4**, 261 (2009).
11. Z. Liu, J.T. Robinson, S.M. Tabakman, K. Yang, and H. Dai: Carbon materials for drug delivery & cancer therapy. *Mater. Today* **14**(7–8), 316 (2011).
12. L. Feng and Z. Liu: Graphene in biomedicine: Opportunities and challenges. *Nanomed.* **6**(2), 317 (2011).
13. H. Shen, L. Zhang, M. Liu, and Z. Zhang: Biomedical applications of graphene. *Theranostics* **2**(3), 283 (2012).
14. D. Jariwala, V.K. Sangwan, L.J. Lauhon, T.J. Marks, and M.C. Hersam: Carbon nanomaterials for electronics, optoelectronics, photovoltaics, and sensing. *Chem. Soc. Rev.* **42**(7), 2824 (2013).
15. C. Fisher, A.E. Rider, Z. Jun Han, S. Kumar, I. Levchenko, and K. (Ken) Ostrikov: Applications and nanotoxicity of carbon nanotubes and graphene in biomedicine. *J. Nanomater.* **2012**, e315185 (2012).
16. K. Yang, L. Feng, X. Shi, and Z. Liu: Nano-graphene in biomedicine: Theranostic applications. *Chem. Soc. Rev.* **42**(2), 530 (2013).
17. H.Y. Mao, S. Laurent, W. Chen, O. Akhavan, M. Imani, A.A. Ashkarran, and M. Mahmoudi: Graphene: Promises, facts, opportunities, and challenges in nanomedicine. *Chem. Rev.* **113**(5), 3407 (2013).
18. Y. Yang, A.M. Asiri, Z. Tang, D. Du, and Y. Lin: Graphene based materials for biomedical applications. *Mater. Today* **16**(10), 365 (2013).
19. C. Chung, Y-K. Kim, D. Shin, S-R. Ryoo, B.H. Hong, and D-H. Min: Biomedical applications of graphene and graphene oxide. *Acc. Chem. Res.* **46**(10), 2211 (2013).
20. G. Hong, S. Diao, A.L. Antaris, and H. Dai: Carbon nanomaterials for biological imaging and nanomedicinal therapy. *Chem. Rev.* **115**(19), 10816 (2015).
21. Z. Li, Z. Liu, H. Sun, and C. Gao: Superstructured assembly of nanocarbons: Fullerenes, nanotubes, and graphene. *Chem. Rev.* **115**(15), 7046 (2015).
22. A.M. Schrand: Perspectives on Carbon Nanomaterials in Medicine Based upon Physicochemical Properties: Nanotubes, Nanodiamonds, and Carbon Nanobombs. In *Carbon Nanomaterials for Biomedical Applications*, M. Zhang, R.R. Naik, and L. Dai, eds. (Springer International Publishing, Cham, 2016); ch. 1, pp. 3–29.
23. C.J. Serpell, K. Kostarelos, and B.G. Davis: Can carbon nanotubes deliver on their promise in biology? Harnessing unique properties for unparalleled applications. *ACS Cent. Sci.* **2**(4), 190 (2016).
24. G.A. Olah, I. Bucsi, R. Aniszfeld, and G.K. Surya Prakash: Chemical reactivity and functionalization of C_{60} and C_{70} fullerenes. *Carbon* **30**(8), 1203 (1992).
25. F. Diederich and M. Gómez-López: Supramolecular fullerene chemistry. *Chem. Soc. Rev.* **28**(5), 263 (1999).
26. K.M. Kadish and R.S. Ruoff, eds.: *Fullerenes: Chemistry, Physics, and Technology* (John Wiley & Sons, Hoboken, 2000).
27. J.M. Englert, C. Dotzer, G. Yang, M. Schmid, C. Papp, J.M. Gottfried, H-P. Steinrück, E. Spiecker, F. Hauke, and A. Hirsch: Covalent bulk functionalization of graphene. *Nat. Chem.* **3**(4), 279 (2011).
28. V. Georgakilas, M. Otyepka, A.B. Bourlinos, V. Chandra, N. Kim, K.C. Kemp, P. Hobza, R. Zboril, and K.S. Kim: Functionalization of graphene: Covalent and non-covalent approaches, derivatives and applications. *Chem. Rev.* **112**(11), 6156 (2012).
29. T. Kuila, S. Bose, A.K. Mishra, P. Khanra, N.H. Kim, and J.H. Lee: Chemical functionalization of graphene and its applications. *Prog. Mater. Sci.* **57**(7), 1061 (2012).
30. T. Nezakati, A. Tan, and A. Seifalian: Different Functionalization Methods of Carbon-based Nanomaterials. In *Chemical Functionalization of Carbon Nanomaterials: Structure and Chemistry*, V.K. Thakur and M.K. Thakur, eds. (CRC Press, Boca Raton, 2015); ch. 2, pp. 28–57.
31. D. Iannazzo, A. Pistone, and S. Galvagno: Functionalization Methods of Graphene. In *Chemical Functionalization of Carbon Nanomaterials: Structure and Chemistry*, V.K. Thakur and M.K. Thakur, eds. (CRC Press, Boca Raton, 2015); ch. 21, pp. 510–537.
32. H. Yi, D. Ghosh, M-H. Ham, J. Qi, P.W. Barone, M.S. Strano, and A.M. Belcher: M13 phage-functionalized single-walled carbon nanotubes as nanoprobes for second near-infrared

window fluorescence imaging of targeted tumors. *Nano Lett.* **12**(3), 1176 (2012).

33. D. Ghosh, A.F. Bagley, Y.J. Na, M.J. Birrer, S.N. Bhatia, and A.M. Belcher: Deep, noninvasive imaging and surgical guidance of submillimeter tumors using targeted M13-stabilized single-walled carbon nanotubes. *Proc. Natl. Acad. Sci.* **111**(38), 13948 (2014).

34. N.M. Bardhan, D. Ghosh, and A.M. Belcher: Carbon nanotubes as *in vivo* bacterial probes. *Nat. Commun.* **5**, 4918 (2014).

35. G-Y. Chen, Z. Li, C.S. Theile, N.M. Bardhan, P.V. Kumar, J.N. Duarte, T. Maruyama, A. Rashidfarrokh, A.M. Belcher, and H.L. Ploegh: Graphene oxide nanosheets modified with single-domain antibodies for rapid and efficient capture of cells. *Chem.–Eur. J.* **21**(48), 17178 (2015).

36. R.S. Ruoff, D.S. Tse, R. Malhotra, and D.C. Lorents: Solubility of fullerene (C_{60}) in a variety of solvents. *J. Phys. Chem.* **97**(13), 3379 (1993).

37. A.K. Manna and S.K. Pati: Computational studies on non-covalent interactions of carbon and boron fullerenes with graphene. *ChemPhysChem* **14**(9), 1844 (2013).

38. S. Jung, J. Seo, and S.K. Shin: Noncovalent binding between fullerenes and protonated porphyrins in the gas phase. *J. Phys. Chem. A* **114**(43), 11376 (2010).

39. S-L. Teh, D. Linton, B. Sumpter, and M.D. Dadmun: Controlling non-covalent interactions to modulate the dispersion of fullerenes in polymer nanocomposites. *Macromolecules* **44**(19), 7737 (2011).

40. F. Li, K.G. Yager, N.M. Dawson, Y-B. Jiang, K.J. Malloy, and Y. Qin: Stable and controllable polymer/fullerene composite nanofibers through cooperative noncovalent interactions for organic photovoltaics. *Chem. Mater.* **26**(12), 3747 (2014).

41. B.K. Reddy, S.C. Gadekar, and V.G. Anand: Non-covalent composites of antiaromatic isophlorin–fullerene. *Chem. Commun.* **51**(39), 8276 (2015).

42. V.A. Basiuk and E. González-Luciano: Noncovalent interactions of amino acids with fullerene C_{60}: A dispersion-corrected DFT study. *Fullerenes, Nanotubes, Carbon Nanostruct.* **24**(6), 371 (2016).

43. F. Diederich and C. Thilgen: Covalent fullerene chemistry. *Science* **271**(5247), 317 (1996).

44. J.M. Hawkins, A. Meyer, T.A. Lewis, S. Loren, and F.J. Hollander: Crystal structure of osmylated C_{60}: Confirmation of the soccer ball framework. *Science* **252**(5003), 312 (1991).

45. R. Injac, M. Perse, M. Cerne, N. Potocnik, N. Radic, B. Govedarica, A. Djordjevic, A. Cerar, and B. Strukelj: Protective effects of fullerenol $C_{60}(OH)_{24}$ against doxorubicin-induced cardiotoxicity and hepatotoxicity in rats with colorectal cancer. *Biomaterials* **30**(6), 1184 (2009).

46. P. Chaudhuri, A. Paraskar, S. Soni, R.A. Mashelkar, and S. Sengupta: Fullerenol−cytotoxic conjugates for cancer chemotherapy. *ACS Nano* **3**(9), 2505 (2009).

47. R. Partha, L.R. Mitchell, J.L. Lyon, P.P. Joshi, and J.L. Conyers: Buckysomes: Fullerene-based nanocarriers for hydrophobic molecule delivery. *ACS Nano* **2**(9), 1950 (2008).

48. J-H. Liu, L. Cao, P.G. Luo, S-T. Yang, F. Lu, H. Wang, M.J. Meziani, S.A. Haque, Y. Liu, S. Lacher, and Y-P. Sun: Fullerene-conjugated doxorubicin in cells. *ACS Appl. Mater. Interfaces* **2**(5), 1384 (2010).

49. E. Nakamura, H. Isobe, N. Tomita, M. Sawamura, S. Jinno, and H. Okayama: Functionalized fullerene as an artificial vector for transfection. *Angew. Chem., Int. Ed.* **39**(23), 4254 (2000).

50. R. Maeda-Mamiya, E. Noiri, H. Isobe, W. Nakanishi, K. Okamoto, K. Doi, T. Sugaya, T. Izumi, T. Homma, and E. Nakamura: *In vivo* gene delivery by cationic tetraamino fullerene. *Proc. Natl. Acad. Sci.* **107**(12), 5339 (2010).

51. H. Tokuyama, S. Yamago, E. Nakamura, T. Shiraki, and Y. Sugiura: Photoinduced biochemical activity of fullerene carboxylic acid. *J. Am. Chem. Soc.* **115**(17), 7918 (1993).

52. J. Liu, S. Ohta, A. Sonoda, M. Yamada, M. Yamamoto, N. Nitta, K. Murata, and Y. Tabata: Preparation of PEG-conjugated fullerene containing Gd^{3+} ions for photodynamic therapy. *J. Controlled Release* **117**(1), 104 (2007).

53. P. Mroz, G.P. Tegos, H. Gali, T. Wharton, T. Sarna, and M.R. Hamblin: Photodynamic therapy with fullerenes. *Photochem. Photobiol. Sci.* **6**(11), 1139 (2007).

54. D.E.J.G.J. Dolmans, D. Fukumura, and R.K. Jain: Photodynamic therapy for cancer. *Nat. Rev. Cancer* **3**(5), 380 (2003).

55. A.M. Smith, M.C. Mancini, and S. Nie: Bioimaging: Second window for *in vivo* imaging. *Nat. Nanotechnol.* **4**(11), 710 (2009).

56. M. Mikawa, H. Kato, M. Okumura, M. Narazaki, Y. Kanazawa, N. Miwa, and H. Shinohara: Paramagnetic water-soluble metallofullerenes having the highest relaxivity for MRI contrast agents. *Bioconjugate Chem.* **12**(4), 510 (2001).

57. R.D. Bolskar, A.F. Benedetto, L.O. Husebo, R.E. Price, E.F. Jackson, S. Wallace, L.J. Wilson, and J.M. Alford: First soluble $M@C_{60}$ derivatives provide enhanced access to metallofullerenes and permit *in vivo* evaluation of $Gd@C_{60}[C(COOH)_2]_{10}$ as a MRI contrast agent. *J. Am. Chem. Soc.* **125**(18), 5471 (2003).

58. B. Sitharaman, R.D. Bolskar, I. Rusakova, and L.J. Wilson: $Gd@C_{60}[C(COOH)_2]_{10}$ and $Gd@C_{60}(OH)_x$: nanoscale aggregation studies of two metallofullerene MRI contrast agents in aqueous solution. *Nano Lett.* **4**(12), 2373 (2004).

59. S. Stevenson, G. Rice, T. Glass, K. Harich, F. Cromer, M.R. Jordan, J. Craft, E. Hadju, R. Bible, M.M. Olmstead, K. Maitra, A.J. Fisher, A.L. Balch, and H.C. Dorn: Small-bandgap endohedral metallofullerenes in high yield and purity. *Nature* **401**(6748), 55 (1999).

60. P.P. Fatouros, F.D. Corwin, Z-J. Chen, W.C. Broaddus, J.L. Tatum, B. Kettenmann, Z. Ge, H.W. Gibson, J.L. Russ, A.P. Leonard, J.C. Duchamp, and H.C. Dorn: *In vitro* and *in vivo* imaging studies of a new endohedral metallofullerene nanoparticle. *Radiology* **240**(3), 756 (2006).

61. J. Zhang, P.P. Fatouros, C. Shu, J. Reid, L.S. Owens, T. Cai, H.W. Gibson, G.L. Long, F.D. Corwin, Z-J. Chen, and H.C. Dorn: High relaxivity trimetallic nitride (Gd_3N) metallofullerene MRI contrast agents with optimized functionality. *Bioconjugate Chem.* **21**(4), 610 (2010).

62. T. Wharton and L.J. Wilson: Highly-iodinated fullerene as a contrast agent for x-ray imaging. *Bioorg. Med. Chem.* **10**(11), 3545 (2002).

63. M.J. O'Connell, S.M. Bachilo, C.B. Huffman, V.C. Moore, M.S. Strano, E.H. Haroz, K.L. Rialon, P.J. Boul, W.H. Noon, C. Kittrell, J. Ma, R.H. Hauge, R.B. Weisman, and R.E. Smalley: Band gap fluorescence from individual single-walled carbon nanotubes. *Science* **297**(5581), 593 (2002).

64. V.C. Moore, M.S. Strano, E.H. Haroz, R.H. Hauge, R.E. Smalley, J. Schmidt, and Y. Talmon: Individually suspended single-walled carbon nanotubes in various surfactants. *Nano Lett.* **3**(10), 1379 (2003).

65. L. Vaisman, H.D. Wagner, and G. Marom: The role of surfactants in dispersion of carbon nanotubes. *Adv. Colloid Interface Sci.* **128–130**, 37 (2006).

66. R.A. Sperling and W.J. Parak: Surface modification, functionalization and bioconjugation of colloidal inorganic nanoparticles. *Philos. Trans. R. Soc. London, Ser. A* **368**(1915), 1333 (2010).

67. J. Cheng, B.A. Teply, I. Sherifi, J. Sung, G. Luther, F.X. Gu, E. Levy-Nissenbaum, A.F. Radovic-Moreno, R. Langer, and O.C. Farokhzad: Formulation of functionalized PLGA–PEG

124

J. Mater. Res., Vol. 32, No. 1, Jan 13, 2017

nanoparticles for *in vivo* targeted drug delivery. *Biomaterials* **28**(5), 869 (2007).

68. B. Dubertret, P. Skourides, D.J. Norris, V. Noireaux, A.H. Brivanlou, and A. Libchaber: *In vivo* imaging of quantum dots encapsulated in phospholipid micelles. *Science* **298**(5599), 1759 (2002).

69. R. Gref, M. Lück, P. Quellec, M. Marchand, E. Dellacherie, S. Harnisch, T. Blunk, and R.H. Müller: "Stealth" corona-core nanoparticles surface modified by polyethylene glycol (PEG): Influences of the corona (PEG chain length and surface density) and of the core composition on phagocytic uptake and plasma protein adsorption. *Colloids Surf., B* **18**(3–4), 301 (2000).

70. K. Welsher, Z. Liu, S.P. Sherlock, J.T. Robinson, Z. Chen, D. Daranciang, and H. Dai: A route to brightly fluorescent carbon nanotubes for near-infrared imaging in mice. *Nat. Nanotechnol.* **4**(11), 773 (2009).

71. K. Welsher, S.P. Sherlock, and H. Dai: Deep-tissue anatomical imaging of mice using carbon nanotube fluorophores in the second near-infrared window. *Proc. Natl. Acad. Sci.* **108**(22), 8943 (2011).

72. J.T. Robinson, G. Hong, Y. Liang, B. Zhang, O.K. Yaghi, and H. Dai: *In vivo* fluorescence imaging in the second near-infrared window with long circulating carbon nanotubes capable of ultrahigh tumor uptake. *J. Am. Chem. Soc.* **134**(25), 10664 (2012).

73. G. Hong, J.C. Lee, J.T. Robinson, U. Raaz, L. Xie, N.F. Huang, J.P. Cooke, and H. Dai: Multifunctional *in vivo* vascular imaging using near-infrared II fluorescence. *Nat. Med.* **18**(12), 1841 (2012).

74. A.L. Antaris, J.T. Robinson, O.K. Yaghi, G. Hong, S. Diao, R. Luong, and H. Dai: Ultra-low doses of chirality sorted (6,5) carbon nanotubes for simultaneous tumor imaging and photothermal therapy. *ACS Nano* **7**(4), 3644 (2013).

75. G. Hong, J.C. Lee, A. Jha, S. Diao, K.H. Nakayama, L. Hou, T.C. Doyle, J.T. Robinson, A.L. Antaris, H. Dai, J.P. Cooke, and N.F. Huang: Near-infrared II fluorescence for imaging hindlimb vessel regeneration with dynamic tissue perfusion measurement. *Circ. Cardiovasc. Imaging* **7**(3), 517 (2014).

76. G. Hong, S. Diao, J. Chang, A.L. Antaris, C. Chen, B. Zhang, S. Zhao, D.N. Atochin, P.L. Huang, K.I. Andreasson, C.J. Kuo, and H. Dai: Through-skull fluorescence imaging of the brain in a new near-infrared window. *Nat. Photonics* **8**(9), 723 (2014).

77. Z. Liu, X. Sun, N. Nakayama-Ratchford, and H. Dai: Supramolecular chemistry on water-soluble carbon nanotubes for drug loading and delivery. *ACS Nano* **1**(1), 50 (2007).

78. S. Dhar, Z. Liu, J. Thomale, H. Dai, and S.J. Lippard: Targeted single-wall carbon nanotube-mediated Pt(IV) prodrug delivery using folate as a homing device. *J. Am. Chem. Soc.* **130**(34), 11467 (2008).

79. Z. Liu, K. Chen, C. Davis, S. Sherlock, Q. Cao, X. Chen, and H. Dai: Drug delivery with carbon nanotubes for *in vivo* cancer treatment. *Cancer Res.* **68**(16), 6652 (2008).

80. Z. Liu, S.M. Tabakman, Z. Chen, and H. Dai: Preparation of carbon nanotube bioconjugates for biomedical applications. *Nat. Protoc.* **4**(9), 1372 (2009).

81. M. Zheng, A. Jagota, E.D. Semke, B.A. Diner, R.S. Mclean, S.R. Lustig, R.E. Richardson, and N.G. Tassi: DNA-assisted dispersion and separation of carbon nanotubes. *Nat. Mater.* **2**(5), 338 (2003).

82. M. Zheng, A. Jagota, M.S. Strano, A.P. Santos, P. Barone, S.G. Chou, B.A. Diner, M.S. Dresselhaus, R.S. Mclean, G.B. Onoa, G.G. Samsonidze, E.D. Semke, M. Usrey, and D.J. Walls: Structure-based carbon nanotube sorting by sequence-dependent DNA assembly. *Science* **302**(5650), 1545 (2003).

83. M.S. Strano, M. Zheng, A. Jagota, G.B. Onoa, D.A. Heller, P.W. Barone, and M.L. Usrey: Understanding the nature of the DNA-assisted separation of single-walled carbon nanotubes

84. X. Huang, R.S. Mclean, and M. Zheng: High-resolution length sorting and purification of DNA-wrapped carbon nanotubes by size-exclusion chromatography. *Anal. Chem.* **77**(19), 6225 (2005).

85. M. Zheng and E.D. Semke: Enrichment of single chirality carbon nanotubes. *J. Am. Chem. Soc.* **129**(19), 6084 (2007).

86. D.P. Salem, M.P. Landry, G. Bisker, J. Ahn, S. Kruss, and M.S. Strano: Chirality dependent corona phase molecular recognition of DNA-wrapped carbon nanotubes. *Carbon* **97**, 147 (2016).

87. X. Tu, S. Manohar, A. Jagota, and M. Zheng: DNA sequence motifs for structure-specific recognition and separation of carbon nanotubes. *Nature* **460**(7252), 250 (2009).

88. J-H. Kim, D.A. Heller, H. Jin, P.W. Barone, C. Song, J. Zhang, L.J. Trudel, G.N. Wogan, S.R. Tannenbaum, and M.S. Strano: The rational design of nitric oxide selectivity in single-walled carbon nanotube near-infrared fluorescence sensors for biological detection. *Nat. Chem.* **1**(6), 473 (2009).

89. N.M. Iverson, P.W. Barone, M. Shandell, L.J. Trudel, S. Sen, F. Sen, V. Ivanov, E. Atolia, E. Farias, T.P. McNicholas, N. Reuel, N.M.A. Parry, G.N. Wogan, and M.S. Strano: *In vivo* biosensing via tissue-localizable near-infrared-fluorescent single-walled carbon nanotubes. *Nat. Nanotechnol.* **8**(11), 873 (2013).

90. Z.W. Ulissi, F. Sen, X. Gong, S. Sen, N. Iverson, A.A. Boghossian, L.C. Godoy, G.N. Wogan, D. Mukhopadhyay, and M.S. Strano: Spatiotemporal intracellular nitric oxide signaling captured using internalized, near-infrared fluorescent carbon nanotube nanosensors. *Nano Lett.* **14**(8), 4887 (2014).

91. N.M. Iverson, G. Bisker, E. Farias, V. Ivanov, J. Ahn, G.N. Wogan, and M.S. Strano: Quantitative tissue spectroscopy of near infrared fluorescent nanosensor implants. *J. Biomed. Nanotechnol.* **12**(5), 1035 (2016).

92. J.P. Giraldo, M.P. Landry, S.M. Faltermeier, T.P. McNicholas, N.M. Iverson, A.A. Boghossian, N.F. Reuel, A.J. Hilmer, F. Sen, J.A. Brew, and M.S. Strano: Plant nanobionics approach to augment photosynthesis and biochemical sensing. *Nat. Mater.* **13**(4), 400 (2014).

93. D. Tasis, N. Tagmatarchis, A. Bianco, and M. Prato: Chemistry of carbon nanotubes. *Chem. Rev.* **106**(3), 1105 (2006).

94. A. Hirsch: Functionalization of single-walled carbon nanotubes. *Angew. Chem., Int. Ed.* **41**(11), 1853 (2002).

95. J. Zhang, H. Zou, Q. Qing, Y. Yang, Q. Li, Z. Liu, X. Guo, and Z. Du: Effect of chemical oxidation on the structure of single-walled carbon nanotubes. *J. Phys. Chem. B* **107**(16), 3712 (2003).

96. P.M. Ajayan, T.W. Ebbesen, T. Ichihashi, S. Iijima, K. Tanigaki, and H. Hiura: Opening carbon nanotubes with oxygen and implications for filling. *Nature* **362**(6420), 522 (1993).

97. K. Tohji, T. Goto, H. Takahashi, Y. Shinoda, N. Shimizu, B. Jeyadevan, I. Matsuoka, Y. Saito, A. Kasuya, T. Ohsuna, K. Hiraga, and Y. Nishina: Purifying single-walled nanotubes. *Nature* **383**(6602), 679 (1996).

98. K.J. Ziegler, Z. Gu, H. Peng, E.L. Flor, R.H. Hauge, and R.E. Smalley: Controlled oxidative cutting of single-walled carbon nanotubes. *J. Am. Chem. Soc.* **127**(5), 1541 (2005).

99. V. Datsyuk, M. Kalyva, K. Papagelis, J. Parthenios, D. Tasis, A. Siokou, I. Kallitsis, and C. Galiotis: Chemical oxidation of multiwalled carbon nanotubes. *Carbon* **46**(6), 833 (2008).

100. N.W.S. Kam, M. O'Connell, J.A. Wisdom, and H. Dai: Carbon nanotubes as multifunctional biological transporters and near-infrared agents for selective cancer cell destruction. *Proc. Natl. Acad. Sci. U. S. A.* **102**(33), 11600 (2005).

101. C. Klumpp, K. Kostarelos, M. Prato, and A. Bianco: Functionalized carbon nanotubes as emerging nanovectors for the delivery of therapeutics. *Biochim. Biophys. Acta, Biomembr.* **1758**(3), 404 (2006).

102. J. Chen, S. Chen, X. Zhao, L.V. Kuznetsova, S.S. Wong, and I. Ojima: Functionalized single-walled carbon nanotubes as rationally designed vehicles for tumor-targeted drug delivery. *J. Am. Chem. Soc.* **130**(49), 16778 (2008).

103. X. Zhang, L. Meng, Q. Lu, Z. Fei, and P.J. Dyson: Targeted delivery and controlled release of doxorubicin to cancer cells using modified single wall carbon nanotubes. *Biomaterials* **30**(30), 6041 (2009).

104. M. Pescatori, D. Bedognetti, E. Venturelli, C. Ménard-Moyon, C. Bernardini, E. Muresu, A. Piana, G. Maida, R. Manetti, F. Sgarrella, A. Bianco, and L.G. Delogu: Functionalized carbon nanotubes as immunomodulator systems. *Biomaterials* **34**(18), 4395 (2013).

105. P.C.B. de Faria, L.I. dos Santos, J.P. Coelho, H.B. Ribeiro, M.A. Pimenta, L.O. Ladeira, D.A. Gomes, C.A. Furtado, and R.T. Gazzinelli: Oxidized multiwalled carbon nanotubes as antigen delivery system to promote superior CD^{8+} T cell response and protection against cancer. *Nano Lett.* **14**(9), 5458 (2014).

106. S. Fedeli, A. Brandi, L. Venturini, P. Chiarugi, E. Giannoni, P. Paoli, D. Corti, G. Giambastiani, G. Tuci, and S. Cicchi: The "click-on-tube" approach for the production of efficient drug carriers based on oxidized multi-walled carbon nanotubes. *J. Mater. Chem. B* **4**(21), 3823 (2016).

107. N. Tsubokawa: Preparation and properties of polymer-grafted carbon nanotubes and nanofibers. *Polym. J.* **37**(9), 637 (2005).

108. S. Ravindran, S. Chaudhary, B. Colburn, M. Ozkan, and C.S. Ozkan: Covalent coupling of quantum dots to multiwalled carbon nanotubes for electronic device applications. *Nano Lett.* **3**(4), 447 (2003).

109. K. Fu, W. Huang, Y. Lin, L.A. Riddle, D.L. Carroll, and Y-P. Sun: Defunctionalization of functionalized carbon nanotubes. *Nano Lett.* **1**(8), 439 (2001).

110. G. Viswanathan, N. Chakrapani, H. Yang, B. Wei, H. Chung, K. Cho, C.Y. Ryu, and P.M. Ajayan: Single-step *in situ* synthesis of polymer-grafted single-wall nanotube composites. *J. Am. Chem. Soc.* **125**(31), 9258 (2003).

111. S. Qin, D. Qin, W.T. Ford, D.E. Resasco, and J.E. Herrera: Polymer brushes on single-walled carbon nanotubes by atom transfer radical polymerization of *n*-butyl methacrylate. *J. Am. Chem. Soc.* **126**(1), 170 (2004).

112. S. Qin, D. Qin, W.T. Ford, D.E. Resasco, and J.E. Herrera: Functionalization of single-walled carbon nanotubes with polystyrene via grafting to and grafting from methods. *Macromolecules* **37**(3), 752 (2004).

113. S. Wang, E.S. Humphreys, S-Y. Chung, D.F. Delduco, S.R. Lustig, H. Wang, K.N. Parker, N.W. Rizzo, S. Subramoney, Y-M. Chiang, and A. Jagota: Peptides with selective affinity for carbon nanotubes. *Nat. Mater.* **2**(3), 196 (2003).

114. D. Pantarotto, C.D. Partidos, R. Graff, J. Hoebeke, J-P. Briand, M. Prato, and A. Bianco: Synthesis, structural characterization, and immunological properties of carbon nanotubes functionalized with peptides. *J. Am. Chem. Soc.* **125**(20), 6160 (2003).

115. J. Montenegro, C. Vázquez-Vázquez, A. Kalinin, K.E. Geckeler, and J.R. Granja: Coupling of carbon and peptide nanotubes. *J. Am. Chem. Soc.* **136**(6), 2484 (2014).

116. D. Pantarotto, C.D. Partidos, J. Hoebeke, F. Brown, E. Kramer, J-P. Briand, S. Muller, M. Prato, and A. Bianco: Immunization with peptide-functionalized carbon nanotubes enhances virus-specific neutralizing antibody responses. *Chem. Biol.* **10**(10), 961 (2003).

117. A. Battigelli, J. Russier, E. Venturelli, C. Fabbro, V. Petronilli, P. Bernardi, T.D. Ros, M. Prato, and A. Bianco: Peptide-based carbon nanotubes for mitochondrial targeting. *Nanoscale* **5**(19), 9110 (2013).

118. K. Kostarelos, L. Lacerda, C.D. Partidos, M. Prato, and A. Bianco: Carbon nanotube-mediated delivery of peptides and genes to cells: Translating nanobiotechnology to therapeutics. *J. Drug Delivery Sci. Technol.* **15**(1), 41 (2005).

119. D.A. Heller, G.W. Pratt, J. Zhang, N. Nair, A.J. Hansborough, A.A. Boghossian, N.F. Reuel, P.W. Barone, and M.S. Strano: Peptide secondary structure modulates single-walled carbon nanotube fluorescence as a chaperone sensor for nitroaromatics. *Proc. Natl. Acad. Sci.* **108**(21), 8544 (2011).

120. J.M. Yun, K.N. Kim, J.Y. Kim, D.O. Shin, W.J. Lee, S.H. Lee, M. Lieberman, and S.O. Kim: DNA origami nanopatterning on chemically modified graphene. *Angew. Chem., Int. Ed.* **51**(4), 912 (2012).

121. N. Mohanty and V. Berry: Graphene-based single-bacterium resolution biodevice and DNA Transistor: Interfacing graphene derivatives with nanoscale and microscale biocomponents. *Nano Lett.* **8**(12), 4469 (2008).

122. A.J. Patil, J.L. Vickery, T.B. Scott, and S. Mann: Aqueous stabilization and self-assembly of graphene sheets into layered bio-nanocomposites using DNA. *Adv. Mater.* **21**(31), 3159 (2009).

123. J. Liu, Y. Li, Y. Li, J. Li, and Z. Deng: Noncovalent DNA decorations of graphene oxide and reduced graphene oxide toward water-soluble metal–carbon hybrid nanostructures via self-assembly. *J. Mater. Chem.* **20**(5), 900 (2010).

124. C-H. Lu, H-H. Yang, C-L. Zhu, X. Chen, and G-N. Chen: A graphene platform for sensing biomolecules. *Angew. Chem., Int. Ed.* **48**(26), 4785 (2009).

125. Y. Xu, Q. Wu, Y. Sun, H. Bai, and G. Shi: Three-dimensional self-assembly of graphene oxide and DNA into multifunctional hydrogels. *ACS Nano* **4**(12), 7358 (2010).

126. M. Wojtoniszak, X. Chen, R.J. Kalenczuk, A. Wajda, J. Łapczuk, M. Kurzewski, M. Drozdzik, P.K. Chu, and E. Borowiak-Palen: Synthesis, dispersion, and cytocompatibility of graphene oxide and reduced graphene oxide. *Colloids Surf., B* **89**, 79 (2012).

127. J.T. Robinson, S.M. Tabakman, Y. Liang, H. Wang, H. Sanchez Casalongue, D. Vinh, and H. Dai: Ultrasmall reduced graphene oxide with high near-infrared absorbance for photothermal therapy. *J. Am. Chem. Soc.* **133**(17), 6825 (2011).

128. H.J. Yoon, T.H. Kim, Z. Zhang, E. Azizi, T.M. Pham, C. Paoletti, J. Lin, N. Ramnath, M.S. Wicha, D.F. Hayes, D.M. Simeone, and S. Nagrath: Sensitive capture of circulating tumour cells by functionalized graphene oxide nanosheets. *Nat. Nanotechnol.* **8**(10), 735 (2013).

129. H.J. Yoon, A. Shanker, Y. Wang, M. Kozminsky, Q. Jin, N. Palanisamy, M.L. Burness, E. Azizi, D.M. Simeone, M.S. Wicha, J. Kim, and S. Nagrath: Tunable thermal-sensitive polymer–graphene oxide composite for efficient capture and release of viable circulating tumor cells. *Adv. Mater.* **28**(24), 4891 (2016).

130. B. Gupta, N. Kumar, K. Panda, A.A. Melvin, S. Joshi, S. Dash, and A.K. Tyagi: Effective noncovalent functionalization of poly (ethylene glycol) to reduced graphene oxide nanosheets through γ-radiolysis for enhanced lubrication. *J. Phys. Chem. C* **120**(4), 2139 (2016).

131. P.V. Kumar, N.M. Bardhan, S. Tongay, J. Wu, A.M. Belcher, and J.C. Grossman: Scalable enhancement of graphene oxide properties by thermally driven phase transformation. *Nat. Chem.* **6**(2), 151 (2014).

126

J. Mater. Res., Vol. 32, No. 1, Jan 13, 2017

132. P.V. Kumar, N.M. Bardhan, G-Y. Chen, Z. Li, A.M. Belcher, and J.C. Grossman: New insights into the thermal reduction of graphene oxide: Impact of oxygen clustering. *Carbon* **100**, 90 (2016).

133. Z. Liu, J.T. Robinson, X. Sun, and H. Dai: PEGylated nano-graphene oxide for delivery of water-insoluble cancer drugs. *J. Am. Chem. Soc.* **130**(33), 10876 (2008).

134. K. Yang, S. Zhang, G. Zhang, X. Sun, S-T. Lee, and Z. Liu: Graphene in mice: Ultrahigh *in vivo* tumor uptake and efficient photothermal therapy. *Nano Lett.* **10**(9), 3318 (2010).

135. W. Zhang, Z. Guo, D. Huang, Z. Liu, X. Guo, and H. Zhong: Synergistic effect of chemo-photothermal therapy using PEGylated graphene oxide. *Biomaterials* **32**(33), 8555 (2011).

136. B. Tian, C. Wang, S. Zhang, L. Feng, and Z. Liu: Photothermally enhanced photodynamic therapy delivered by nano-graphene oxide. *ACS Nano* **5**(9), 7000 (2011).

137. J. Cao, H. An, X. Huang, G. Fu, R. Zhuang, L. Zhu, J. Xie, and F. Zhang: Monitoring of the tumor response to nano-graphene oxide-mediated photothermal/photodynamic therapy by diffusion-weighted and BOLD MRI. *Nanoscale* **8**(19), 10152 (2016).

138. L. Feng, X. Yang, X. Shi, X. Tan, R. Peng, J. Wang, and Z. Liu: Polyethylene glycol and polyethylenimine dual-functionalized nano-graphene oxide for photothermally enhanced gene delivery. *Small* **9**(11), 1989 (2013).

139. C. Shan, H. Yang, D. Han, Q. Zhang, A. Ivaska, and L. Niu: Water-soluble graphene covalently functionalized by biocompatible poly-l-lysine. *Langmuir* **25**(20), 12030 (2009).

140. S-H. Hu, Y-W. Chen, W-T. Hung, I-W. Chen, and S-Y. Chen: Quantum-dot-tagged reduced graphene oxide nanocomposites for bright fluorescence bioimaging and photothermal therapy monitored *in situ*. *Adv. Mater.* **24**(13), 1748 (2012).

141. H. Hong, K. Yang, Y. Zhang, J.W. Engle, L. Feng, Y. Yang, T.R. Nayak, S. Goel, J. Bean, C.P. Theuer, T.E. Barnhart, Z. Liu, and W. Cai: *In vivo* targeting and imaging of tumor vasculature with radiolabeled, antibody-conjugated nanographene. *ACS Nano* **6**(3), 2361 (2012).

142. K. Yang, L. Feng, H. Hong, W. Cai, and Z. Liu: Preparation and functionalization of graphene nanocomposites for biomedical applications. *Nat. Protoc.* **8**(12), 2392 (2013).

143. A. Sinitskii, A. Dimiev, D.A. Corley, A.A. Fursina, D.V. Kosynkin, and J.M. Tour: Kinetics of diazonium functionalization of chemically converted graphene nanoribbons. *ACS Nano* **4**(4), 1949 (2010).

144. D.V. Kosynkin, A.L. Higginbotham, A. Sinitskii, J.R. Lomeda, A. Dimiev, B.K. Price, and J.M. Tour: Longitudinal unzipping of carbon nanotubes to form graphene nanoribbons. *Nature* **458**(7240), 872 (2009).

145. S. Niyogi, E. Bekyarova, M.E. Itkis, H. Zhang, K. Shepperd, J. Hicks, M. Sprinkle, C. Berger, C.N. Lau, W.A. deHeer, E.H. Conrad, and R.C. Haddon: Spectroscopy of covalently functionalized graphene. *Nano Lett.* **10**(10), 4061 (2010).

146. R. Sharma, J.H. Baik, C.J. Perera, and M.S. Strano: Anomalously large reactivity of single graphene layers and edges toward electron transfer chemistries. *Nano Lett.* **10**(2), 398 (2010).

147. M.Z. Hossain, M.A. Walsh, and M.C. Hersam: Scanning tunneling microscopy, spectroscopy, and nanolithography of epitaxial graphene chemically modified with aryl moieties. *J. Am. Chem. Soc.* **132**(43), 15399 (2010).

148. H. Liu, S. Ryu, Z. Chen, M.L. Steigerwald, C. Nuckolls, and L.E. Brus: Photochemical reactivity of graphene. *J. Am. Chem. Soc.* **131**(47), 17099 (2009).

149. L. Zhang, J. Xia, Q. Zhao, L. Liu, and Z. Zhang: Functional graphene oxide as a nanocarrier for controlled loading and targeted delivery of mixed anticancer drugs. *Small* **6**(4), 537 (2010).

150. X. Zhang, L. Hou, A. Cnossen, A.C. Coleman, O. Ivashenko, P. Rudolf, B.J. van Wees, W.R. Browne, and B.L. Feringa: One-pot functionalization of graphene with porphyrin through cyclo-addition reactions. *Chem.–Eur. J.* **17**(32), 8957 (2011).

151. G. Wei, M. Yan, R. Dong, D. Wang, X. Zhou, J. Chen, and J. Hao: Covalent modification of reduced graphene oxide by means of diazonium chemistry and use as a drug-delivery system. *Chem.–Eur. J.* **18**(46), 14708 (2012).

152. G. Gollavelli and Y-C. Ling: Multi-functional graphene as an *in vitro* and *in vivo* imaging probe. *Biomaterials* **33**(8), 2532 (2012).

153. A. Servant, A. Bianco, M. Prato, and K. Kostarelos: Graphene for multi-functional synthetic biology: The last "zeitgeist" in nano-medicine. *Bioorg. Med. Chem. Lett.* **24**(7), 1638 (2014).

154. S. Bhaskar, F. Tian, T. Stoeger, W. Kreyling, J.M. de la Fuente, V. Grazú, P. Borm, G. Estrada, V. Ntziachristos, and D. Razansky: Multifunctional nanocarriers for diagnostics, drug delivery and targeted treatment across blood-brain barrier: Perspectives on tracking and neuroimaging. *Part. Fibre Toxicol.* **7**, 3 (2010).

155. K. Momma and F. Izumi: VESTA 3 for three-dimensional visualization of crystal, volumetric and morphology data. *J. Appl. Crystallogr.* **44**(6), 1272 (2011).

156. J.T. Robinson, K. Welsher, S.M. Tabakman, S.P. Sherlock, H. Wang, R. Luong, and H. Dai: High performance *in vivo* near-IR (>1 μm) imaging and photothermal cancer therapy with carbon nanotubes. *Nano Res.* **3**(11), 779 (2010).

157. Z. Yinghuai, A.T. Peng, K. Carpenter, J.A. Maguire, N.S. Hosmane, and M. Takagaki: Substituted carborane-appended water-soluble single-wall carbon nanotubes: new approach to boron neutron capture therapy drug delivery. *J. Am. Chem. Soc.* **127**(27), 9875 (2005).

158. H. Dumortier, S. Lacotte, G. Pastorin, R. Marega, W. Wu, D. Bonifazi, J-P. Briand, M. Prato, S. Muller, and A. Bianco: Functionalized carbon nanotubes are non-cytotoxic and preserve the functionality of primary immune cells. *Nano Lett.* **6**(7), 1522 (2006).

159. W. Tu, J. Lei, S. Zhang, and H. Ju: Characterization, direct electrochemistry, and amperometric biosensing of graphene by noncovalent functionalization with picket-fence porphyrin. *Chem.–Eur. J.* **16**(35), 10771 (2010).

160. S. Zhang, S. Tang, J. Lei, H. Dong, and H. Ju: Functionalization of graphene nanoribbons with porphyrin for electrocatalysis and amperometric biosensing. *J. Electroanal. Chem.* **656**(1–2), 285 (2011).

Supplementary Material

To view supplementary material for this article, please visit https://doi.org/10.1557/jmr.2016.449.